DISSERTATIONES
PHYSICAE
UNIVERSITATIS
TARTUENSIS
134

KRISTJAN MÜÜRSEPP

Phenomenological implications of Standard Model extensions

DISSERTATIONES PHYSICAE UNIVERSITATIS TARTUENSIS
134

DISSERTATIONES PHYSICAE UNIVERSITATIS TARTUENSIS
134

KRISTJAN MÜÜRSEPP

Phenomenological implications of Standard Model extensions

UNIVERSITY OF TARTU
Press
1632

This study was carried out at the National Institute of Chemical Physics and Biophysics, Tallinn, and the University of Tartu, Estonia.

The dissertation was admitted on 12.06.2024 in partial fulfillment of the requirements for the degree of Doctor of Philosophy in physics, and was allowed for defence by the Council of the Institute of Physics, University of Tartu.

Supervisors: Dr. Luca Marzola,
National Institute of Chemical Physics and Biophysics,
Tallinn, Estonia

Dr. Martti Raidal,
National Institute of Chemical Physics and Biophysics,
Tallinn, Estonia

Opponent: Prof. Kimmo Kainulainen
Jyväskylä University,
Jyväskylä, Finland

Defence: September 27, 2024, University of Tartu, Estonia

ISSN 1406-0647 (print)
ISBN 978-9916-27-628-0 (print)
ISSN 2806-2523 (pdf)
ISBN 978-9916-27-629-7 (pdf)

University of Tartu Press
www.tyk.ee

Contents

List of original publications

The results of this Thesis are compiled in the three following research publications:

I. J. C. Criado, A. Djouadi, N. Koivunen, K. Müürsepp, M. Raidal, H. Veermäe, "Confronting spin-3/2 and other new fermions with the muon g-2 measurement",
Phys.Lett.B **820** (2021), arXiv:2104.03231 [hep-ph].

II. E. Gabrielli, L. Marzola, K. Müürsepp, R. Ouyang,
"Vacuum stability with radiative Yukawa couplings",
JHEP **01** (2022) 142, arXiv:2106.09038 [hep-ph].

III. E. Gabrielli, L. Marzola, K. Müürsepp, M. Raidal,
"Explaining the $B^+ \to K^+ \nu\bar{\nu}$ excess via a massless dark photon",
Eur. Phys. J. C, **84** 460 (2024), arXiv:2402.05901 [hep-ph].

Author's contribution

In publication I, the dissertant performed all the analytical and numerical computations for the spin-3/2 case, cross-checked the results for the spin-1/2 case, and prepared the figures. Together with the coauthors, the dissertant contributed to the process of writing the manuscript.

In publication II, the dissertant wrote the first version of the code for computing the beta functions and made changes on the second version of the code written by his supervisor, to effectively use the code to compute the beta functions of the model, performed all the numerical computations, cross-checked the analytical formulae, and prepared all the figures for the paper. Together with the coauthors, the dissertant contributed to the process of writing the manuscript.

In publication III, the dissertant performed all the numerical calculations needed to fit the anomaly, cross-checked the analytical formulae and prepared all the figures. Together with the coauthors, the dissertant contributed to the process of writing the manuscript.

Other publications of the dissertant

I. D. Anselmi, K. Kannike, C. Marzo, L. Marzola, A. Melis, K. Müürsepp, M. Piva, M. Raidal, "Phenomenology of a fake Inert Doublet Model", JHEP **10** (2021), arXiv:2104.02071 [hep-ph].

II. D. Anselmi, K. Kannike, C. Marzo, L. Marzola, A. Melis, K. Müürsepp, M. Piva, M. Raidal, "Fake doublet solution to the muon anomalous magnetic moment", Phys.Rev.D **104** (2021), 035009, arXiv:2104.03249 [hep-ph].

III. J. C. Criado, A. Djouadi, N. Koivunen, K. Müürsepp, M. Raidal, H. Veermäe, "New fermions in the light of the $(g-2)_\mu$ ", Front.in Phys. **10** (2022), 964131, arXiv:2112.12502 [hep-ph].

IV. M. Lewicki, K. Müürsepp, J. Pata, M. Vasar, V. Vaskonen, H. Veermäe, " Dynamics of false vacuum bubbles with trapped particles ", Phys.Rev.D **108** (2023) 3, 036023, arXiv:2305.07702 [hep-ph].

Acknowledgments

First and foremost, I would like to sincerely thank my supervisors Luca Marzola and Martti Raidal, for guiding me throughout the PhD journey by creating a very friendly and informal work environment, for being available for discussions, and for encouraging me to broaden my horizon by working on different areas of physics.

In addition to the advice and leadership of my supervisors, the beginning of my academic journey was also decidedly strengthened by the support of several other colleagues with whom I had the pleasure to collaborate with. Specifically, I would like to pass on my deepest gratitude to Enrico Nardi, whose profound intuition and enthusiasm for physics have strongly influenced my approach to research; Emidio Garielli, who was constantly available for discussions and clarifications while working on our common projects and Niko Koivunen, who has helped me a lot in learning about higher spin theories and who provided me invaluable advice about adapting to an academic lifestyle in the early stages of my PhD.

More generally I would like to thank all of my other colleagues who have helped me immensely while working on shared projects, with whom I have had some fierce games of table-(and real) football or stimulating discussions and who have been the most pleasant of travel companions during conferences and summer schools. Specifically, I would like to mention: Clemente Smarra, Martin Vasar, Ruiwen Ouyang, Ville Vaskonen, Marek Lewicki, Joosep Pata, Aurora Melis, Marco Piva, Kristjan Kannike, Damiano Anselmi, Carlo Marzo, Juan Carlos Criado, Abdelhak Djouadi, Hardi Veermäe, Luigi Delle Rose, Antonio Iovino Junior, Quirijn Meijer, Pierluca Carenza, Carlo Tasillo, Juan Urrutia, Rafal Maselek, Tim Höhne, Aika Tada, Chaja Baruch, Fernando Arias Aragon, Prisco Lo Chiatto, Priidik Gallagher, Juhan Raidal, Pablo Matorras, Christian Dioguardi, Sven Põder, Nico Benincasa, Vinicius Padovani, Giuseppe Lucente, Illaria Andrei, Aula al-Adulrazzaq and Maria Benito.

A special mention to my friends outside of the physics community, whose presence has allowed me to relax and think of other stuff for a change. I wish to pass on the warmest of greetings to Erik, Gustav, Reio, Joosep, Annabel, Kätlin, Laura, Richard, Vladislav, Leonid, Hendrik, Sietse, An-

dres, Aleksander, and all the ballers of our football team Salme Soccer Squad.

Above all, I am indebted to my family, without whom none of this would be possible. My eternal gratitude goes out to Eha, Eike, Mari-Liis, and Aivar for providing me the platform to embark on this fascinating journey and for supporting me throughout, and especially to Natalia whose love and compassion have been an integral component of my academic journey on a daily basis.

This work was supported by the Estonian Research Council grant PRG-803 and Coe TK 202. Additionally, I benefitted from the travel grants offered by Cost Actions CA18108 and CA16201, the joint initiative of ICTP-SAIFR and Mainz summer school, and from the Kristjan Jaak grant for short term visits. I thank the Galileo Galilei Institute and INFN-LNF, where I spent extended periods doing research, for their hospitality.

Chapter 1

Introduction

The Standard Model (SM) of particle physics, formulated a little more than 50 years ago, has proved to be the most accurate theory of elementary interactions. Describing all fundamental forces besides gravity, it has been able to explain a plethora of experimental observations and its predictions have withstood the test of time. In 2012, the discovery of the last missing particle of the SM, the Higgs boson, was reported by the CMS [1] and ATLAS [2] collaborations, decisively establishing the internal self-consistency of the theory. Nevertheless, despite the numerous triumphs of the SM, several open questions remain unanswered, calling for explorations beyond the traditional paradigm.

Though the SM is a self-consistent theory of elementary interactions, it falls short of giving a satisfactory description for several observed phenomena in the Universe. From the cosmological side the SM fails to account for dark matter (DM), a mysterious form of matter that accounts for approximately 27% of the energy budget of the Universe and is a crucial ingredient of the standard cosmological model (ΛCDM) affecting processes such as structure formation, big bang nucleosynthesis and the rotational speed of stars around the centers of galaxies. Moreover, it does not provide a natural explanation for dark energy, which contributes 68% to the total energy budget of the Universe and is responsible for the accelerated expansion of space. Finally, the SM is not sufficient to explain the observed asymmetry between matter and antimatter.

Cosmology aside, there are also conceptual issues related to the existing constituents of the SM, which though not invalidating the theory, should still be addressed in search for a more fundamental description of Nature. The most weakly interacting particles of the SM, the neutrinos, happen to be also the lightest and are thus assumed to have zero mass in the SM. However, through the observations of neutrino oscillations, it has been established that neutrinos do have a non-zero mass, which should be taken

into account by prospective extensions of the SM [3]. In a somewhat related fashion, the hierarchy of all other fermion masses also remains unexplained within the SM, given the fact that this hierarchy results only from the *ad-hoc* tuning of the dimensionless input parameters of the model. Finally, the SM also exhibits several fine-tuning problems such as the Higgs hierarchy problem and the strong CP problem. The former is related to the fact that the Higgs mass is not protected from obtaining huge quantum corrections should the SM hold up to very high energy scales. The latter however is associated with intrinsic parameters of the SM that due to the constraints on the electric dipole moment of the neutron should cancel up to very small values [4]. All of the conceptual issues listed above may be addressed by employing new particles and (or) new symmetries beyond the SM (BSM) to introduce a dynamical mechanism that sets the SM parameters to their observed values. In this case, no fine-tuning is necessary. Historically, two of the most celebrated attempts to tackle some of the issues listed above are supersymmetry (SUSY) [5, 6] and theories of axions [7–9]. Whilst working on these ideas, it was soon discovered that they can often also provide necessary ingredients for ΛCDM such as dark matter [10–12]. Thus it is clear that the cosmological and conceptual deficiencies of the SM can be seen as complementary tools in the search of more fundamental BSM theory.

Given the endless spectrum of possible theories, it is imperative to be constantly on the lookout for hints of new physics (NP) both from the collider experiments and from the cosmos. One possible strategy in the search for NP at colliders is to look for deviations from the SM in decays of heavy mesons. These decays often involve flavour-changing neutral currents (FCNC) that are very strongly suppressed by the Glashow, Iliopoulos, Maiani (GIM) mechanism as reviewed later in this Thesis [13]. Thus, any deviation in the rate of these decays gives a hint of the presence of NP. Secondly, the recently reported deviation of the muon anomalous magnetic moment (g-2) provides another possible direction toward BSM physics [14]. Interestingly, any significant deviation of the muon (g-2) must be caused by particles with masses near or below the electroweak (EW) scale, leading to predictions of new particles within the reach of current collider experiments.

Another possible clue for identifying extensions of the SM is provided by the vacuum structure of the SM. In the SM, all masses of elementary particles are generated once the Higgs field obtains a non-zero background value at the EW scale of 125 GeV known as the EW vacuum expectation value (vev) [15–17]. This vacuum state should be stable or have a long enough lifetime such that the observed structures in our Universe can form and stay intact until the present. Within the SM it turns out that the EW vev of the Higgs boson, responsible for the masses of the elementary parti-

cle, corresponds to a local minimum of the Higgs' potential, with another, deeper minimum appearing at higher field values due to quantum corrections [18]. This, however, does not contradict the observed properties of the elementary particles if the EW vev corresponds to a metastable state with a lifetime longer than the age of the Universe. Hence, in the SM a precise computation of the tunneling rate from the EW vev to another minima at higher field values becomes crucial to determine the stability of the Universe. In this regard, it is interesting to consider models in which the EW vacuum is not metastable but absolutely stable - in other words - where the EW vev corresponds to the global minimum of the Higgs potential. In this case the stability of the Universe is guaranteed.

In this Thesis, we will closely examine different hints of NP such as flavour anomalies, the anomalous magnetic moment of the muon and the vacuum stability in order to motivate extensions of the SM. Though we choose to motivate these models by particular hints of NP, they can also alleviate other shortcomings of the SM by solving the flavour hierarchy problem, providing a dark matter candidate or addressing the Higgs hierarchy problem.

The Thesis is structured as follows. In Chapter 2 we offer a quick review of the SM with particular focus on the Higgs mechanism and the masses of elementary particles. In particular, we will explain the flavour hierarchy problem. Chapter 3 is focused on the stability of the EW vacuum. We highlight the role of the Yukawa couplings on the vacuum stability of the SM and how it may be modified for different models of NP. Chapter 4 details how the magnetic moment of muon is modified by quantum corrections and explains which models of NP may address the recently observed excess with respect to the SM prediction. In Chapter 5 we highlight the role of FCNC as probes of NP, specifically in connection to the flavour anomalies. Finally, in Chapters 6 and 7 we introduce two possible models of NP that address the shortcomings of the SM described in the previous Chapters. A summary of the results can be found from Chapters 8 (in English) and 9 (in Estonian). The papers on which this Thesis is based can be found in the Appendix.

Chapter 2

The Standard Model of particle physics

The SM is a theoretical particle physics model describing the dynamics, masses, and interactions of the matter particles and the force mediators [19–21]. The Lagrangian of the SM is constrained by Lorentz invariance, renormalizability, and local gauge invariance. The first two of these conditions are needed to define finite, frame-independent observables for particle physics processes, while the last condition allows to identify the interaction between the matter particles and the gauge bosons that are responsible for mediating three elementary forces - the strong, weak and electromagnetic force. The corresponding gauge group is a direct product of three Lie groups: $SU(3)_c \times SU(2)_L \times U(1)_Y$, where the subscripts refer to the color, weak isospin and hypercharge quantum numbers respectively [22]. Given that the Lagrangian must be invariant under a local transformation of this gauge group, the derivatives appearing in the kinetic terms of the Lagrangian must be generalized to covariant derivatives [23]. The generalization to covariant derivatives can be easily carried out by using a minimal substitution as follows:

$$\partial_\mu \rightarrow D_\mu = \partial_\mu - ig' B_\mu Y - igW_\mu^a t^a - ig_s G_\mu^b t^b, \tag{2.1}$$

where g', g, g_s are the coupling constants of $U(1)_Y$ and $SU(2)_L$, $SU(3)_c$ respectively. The indices $a = 1, 2, 3$ and $b = 1, .., 8$ identify the basis vectors for the 3- and 8-dimensional Lie algebras of $SU(2)_L$ and $SU(3)_c$. Summation over repeated indices is used here and elsewhere in this Thesis unless explicitly stated otherwise. From hereon, we sometimes refer to the indices a and b as the weak isospin and color indices, respectively.

By imposing the symmetry of the Lagrangian under this gauge group, new bosonic fields of spin 1 are introduced: eight vector fields G_μ^b for $SU(3)_c$, three vector fields W_μ^a for $SU(2)_L$ and one vector field B_μ for $U(1)_Y$. Over-

all, the Lagrangian of the SM is given by [1]

$$\begin{aligned}\mathcal{L} = &-\frac{1}{4}B_{\mu\nu}B^{\mu\nu} - \frac{1}{4}W^a_{\mu\nu}W^{a\mu\nu} - \frac{1}{4}G^b_{\mu\nu}G^{b\mu\nu} \\ &+i\bar{\psi}_{L,i}\not{D}\psi_{L,i} + i\bar{\psi}_{R,i}\not{D}\psi_{R,i} + (D_\mu\phi)^\dagger D^\mu\phi \\ &+\mu^2\phi^\dagger\phi - \lambda_H(\phi^\dagger\phi)^2 + Y_{ij}\bar{\psi}_{L,i}\phi\psi_{R,j} + h.c.,\end{aligned} \tag{2.2}$$

where $a = 1, 2, 3$ and $b = 1, .., 8$, as before, and i, j run over the three generations of the charged leptons and u- and d-type quarks. The first three terms appearing in eq. (2.2) describe the kinetic terms of the B bosons corresponding to the $U(1)_Y$ symmetry known as the hypercharge, the three W bosons of the weak interaction and the eight gluons of the strong interaction. Explicitly one has

$$B_{\mu\nu} = \partial_\mu B_\nu - \partial_\nu B_\mu, \tag{2.3}$$

$$W^a_{\mu\nu} = \partial_\mu W^a_\nu - \partial_\nu W^a_\mu + g f^{abc} W^b_\mu W^c_\nu, \tag{2.4}$$

with $a, b, c = 1, 2, 3$, and

$$G^a_{\mu\nu} = \partial_\mu G^a_\nu - \partial_\nu G^a_\mu + g_s g^{abc} G^b_\mu, \tag{2.5}$$

with $a, b, c = 1, ..8$ [23]. The structure constants f^{abc} and g^{abc} appearing in eqs. (2.4) and (2.5) originate from the corresponding Lie algebras of $SU(2)_L$ and $SU(3)_c$, due to the following relation between the generators of the corresponding Lie algebras t_i for $SU(2)_L$ and t^i_s for $SU(3)_c$:

$$[t^a, t^b] = i f^{abc} t^c, \quad [t^a_s, t^b_s] = i g^{abc} t^c_s. \tag{2.6}$$

The fermions of the SM are described by spin-1/2 spinor fields ψ.[2] The chiral fermion sector consists of the left-handed fields ψ_L transforming as doublets under $SU(2)_L$ and the right-handed fields transforming as singlets under $SU(2)_L$ [20]. The fermion sector of the SM can be subdivided into two classes. The elementary fermions that do not participate in the strong interaction associated with the $SU(3)_c$ group are known as leptons, with the left-handed leptons organized into doublets of $SU(2)_L$ (denoted as L_L) and the right-handed leptons organized into singlets of $SU(2)_L$ (denoted as e_R). The fermions that are subject to the strong interaction are called quarks and transform as triplets of $SU(3)_c$. The representation under the

[1] Here, in order to avoid notational clutter we omit the a and b indices from the scalar and fermion fields.

[2] From hereon the generation, color and weak isospin indices are suppressed for the sake of clarity.

	Q_L	u_R	d_R	L_L	e_R
$U(1)_Y$	$\frac{1}{6}$	$\frac{2}{3}$	$-\frac{1}{3}$	$-\frac{1}{2}$	-1
$SU(2)_L$	$(\frac{1}{2}, -\frac{1}{2})$	0	0	$(\frac{1}{2}, -\frac{1}{2})$	0
$SU(3)_c$	triplet	triplet	triplet	singlet	singlet

Table 2.1: The gauge quantum numbers of the SM fermions.

$SU(2)_L$ group again follows the same logic as above: the left-handed quarks are collected into doublets (denoted as Q_L) and the right-handed quarks appear in singlets (denoted as u_R in case of quarks with positive electric charge and d_R in case of quarks with negative electric charge). The transformation properties of the elementary fermions under the SM gauge group are summarized in Table 2.1.

The first term on the second line of eq. (2.2) is the kinetic term of the fermion fields, where the partial derivative has been replaced by the covariant derivative as described by eq. (2.1) and $\not{D} = D_\mu \gamma^\mu$. Due to this replacement, interaction terms between the fermions and the gauge bosons will appear in the Lagrangian in addition to the kinetic terms of the fermion fields. The strength of these interactions is governed by the gauge coupling constants g', g, g_s associated with $U(1)_Y$, $SU(2)_L$ and $SU(3)_c$ respectively. Moreover, the strength of these three interactions also depends on the energy scale at which physical processes are probed since g, g' and g_s are not really constant but instead "run" with energy as described in Chapter 3. Interestingly, since g_s becomes non-perturbative at low energies, it follows that all particles participating in the strong interaction cannot be observed as free particles and must be, instead, confined into composite, color-neutral states [24–26]. Finally, a complex scalar field ϕ is also included in the SM Lagrangian. This field, known as the Higgs doublet, is used to carry out the spontaneous breaking of the $SU(2)_L \times U(1)_Y$ symmetry. It should be noted that since ϕ is a singlet under the $SU(3)_c$ group the last term of eq. (2.1) does not appear in $(D_\mu \phi)^\dagger D^\mu \phi$. Consequently, the Higgs field ϕ does not interact with gluons. The quadratic and quartic operators in ϕ appearing in eq. (2.2) describe the so-called Higgs potential, which sources the spontaneous symmetry breaking (SSB) in the EW sector, described in Section 2.1. The last term of the SM Lagrangian in eq. (2.2) collects the Yukawa terms responsible for generating the fermion masses after the spontaneous breaking of the EW symmetry. Within the SM the hierarchy in the corresponding Yukawa couplings does not follow from any underlying principle and the values of the couplings are only fixed by experiments.

2.1 The Higgs mechanism

It is evident from eq. (2.2) that the SM Lagrangian contains no mass terms for the elementary fermions nor gauge bosons. This is because mass terms for these fields would explicitly break local gauge invariance under the SM gauge group. To overcome this issue, the gauge symmetry can be instead broken spontaneously thereby generating the required mass terms. To that end we can employ a scalar field ϕ introduced in the previous Section, which spontaneously breaks the $SU(2)_L \times U(1)_Y$ symmetry[3] [15–17]. The scalar field ϕ can be written as follows:

$$\phi = \frac{1}{\sqrt{2}} \begin{pmatrix} \phi_1 + i\phi_2 \\ \phi_3 + i\phi_4 \end{pmatrix}. \tag{2.7}$$

It is a color singlet, a $SU(2)_L$ doublet with hypercharge $Y = 1/2$ and it appears in the Lagrangian of the SM as described in eq. (2.2). In particular, the sum of the first two terms on the third line of eq. (2.2) defines the Higgs potential $V(\phi)$ whose parametric form is of crucial importance for the symmetry-breaking mechanism. Explicitly we have

$$V(\phi) = -\mu_H^2 \phi^\dagger \phi + \lambda_H \left(\phi^\dagger \phi\right)^2. \tag{2.8}$$

Higher powers of ϕ are omitted on the grounds of renormalizability. The potential in eq. (2.8) can have minima at different values of field space depending on the values of μ_H and λ_H. These minima define the vacuum of the theory and the corresponding vev-s: $v = \sqrt{\langle \phi^\dagger \phi \rangle}$. In particular, there are three distinct options:

1. If $\lambda_H < 0$, the potential is not bounded from below and there is no stable vacuum state.

2. When $\lambda_H > 0$ and $-\mu_H^2 > 0$, the minimum energy state is given by $\langle \phi \rangle = 0$. In that case, the vacuum state given by $\langle \phi \rangle = 0$ is unchanged under a gauge transformation of the $SU(2)_L \times U(1)_Y$ group, and hence the $SU(2)_L \times U(1)_Y$ symmetry remains unbroken.

3. Finally, if $\lambda_H > 0$ and $-\mu_H^2 < 0$, it can be easily seen that the minimum energy configuration is given by

$$\left\langle \phi^\dagger \phi \right\rangle = \frac{\mu_H^2}{2\lambda_H}. \tag{2.9}$$

   In that case, the $SU(2)_L \times U(1)_Y$ gauge symmetry has been spontaneously broken and ϕ obtains an expectation value, given by eq. (2.9).

[3] This $SU(2)_L \times U(1)_Y$ symmetry breaking mechanism is usually referred to as the Higgs mechanism.

Given that ϕ is a $SU(2)_L \times U(1)_Y$ doublet and $SU(3)_c$ singlet, a general transformation of the SM gauge group on ϕ can be written as

$$\phi(x) \to \phi e^{i\left(\alpha_j(x))\frac{\sigma_j}{2}+\beta(x)\frac{Y}{2}\right)}, \tag{2.10}$$

where σ_j and Y are the generators of the Lie algebras of $SU(2)_L$ and $U(1)_Y$ and $\alpha_j(x)$ and $\beta(x)$ are the corresponding expansion coefficients. Moreover, the 4 components of the complex doublet $\phi(x)$ can be conveniently parametrized as

$$\phi(x) = e^{i\pi_j(x)\frac{\sigma^j}{2}} \begin{pmatrix} 0 \\ \frac{v+h(x)}{\sqrt{2}} \end{pmatrix}, \tag{2.11}$$

where $\pi_j(x)$ is a scalar function of the spacetime coordinates, v is the vev of ϕ and $h(x)$ is a small excitation of the vacuum known as the Higgs boson. Then by performing a $SU(2)$ gauge transformation, choosing $\alpha_j(x) = -\pi_j(x)$ and $\beta(x) = 0$ in eq. (2.10) we can bring ϕ to a simpler form as shown below,

$$\phi(x) = \frac{1}{\sqrt{2}} \begin{pmatrix} 0 \\ h(x) + v \end{pmatrix}. \tag{2.12}$$

This gauge is known as the unitary gauge. Expressing ϕ in this gauge, we see explicitly that only one degree of freedom of ϕ corresponds to a physical, propagating particle. The rest of the degrees of freedom, known as the Goldstone bosons [27] end up becoming the longitudinal modes of the three gauge bosons of $SU(2)_L \times U(1)_Y$, denoted by W^+, W^-, Z which consequently become massive fields. There is still one gauge boson of $SU(2)_L \times U(1)_Y$ that remains massless, since after the breaking of $SU(2)_L \times U(1)_Y$ a residual $U(1)_{EM}$ symmetry associated with electromagnetism remains unbroken. The remaining massless field can be identified with the photon. Rewriting eq. (2.8) in the unitary gauge and eliminating $\mu_H^2 = \lambda_H v^2$ gives

$$V(\phi) = const + \frac{1}{2}\lambda_H v^2 h^2 + \frac{1}{2\sqrt{2}}\lambda_H v h^3 + \frac{\lambda_H}{4} h^4. \tag{2.13}$$

It follows directly that the mass of h is given by

$$m_h = \sqrt{\lambda_H v^2}. \tag{2.14}$$

2.2 The fermion masses and mixing

As mentioned in the previous Section, due to the requirement of local gauge invariance, fermion masses can only be generated via SSB of the EW symmetry by coupling the fermions to the Higgs field [19, 28]. The

coupling constants controlling this interaction are known as Yukawa couplings, and the corresponding interaction is shown explicitly in eq. (2.2). To explore the mechanism in more detail, let us start from charged leptons. The Yukawa terms in the Lagrangian,[4] responsible for the generation of the lepton masses are given by [22, 29]

$$\mathcal{L}^{l}_{Yuk} = -\sum_{i,j=e,\mu,\tau} \left(y_{ij} \bar{e'}_{iR} \phi^{\dagger} L'_{jL} + y^{*}_{ij} \bar{L}'_{jL} \phi e'_{iR} \right). \tag{2.15}$$

Employing the unitary gauge, eq. (2.15) can be recast as

$$\mathcal{L}^{l}_{Yuk} = -\sum_{i,j=e,\mu,\tau} \frac{1}{\sqrt{2}} \left[(v+h)\, y_{ij} \bar{e'}_{iR} e'_{jL} + (v+h)\, y^{*}_{ij} \bar{e'}_{jL} e'_{iR} \right]. \tag{2.16}$$

Manifestly, the mass matrix for the charged leptons is proportional to the Yukawa matrix and thus the physical masses are given by the rescaled eigenvalues of the Yukawa matrix

$$m_i = \frac{y_i v}{\sqrt{2}}, \qquad i = 1, 2, 3, \tag{2.17}$$

where y_i denote the $i-$th eigenvalue.

For quarks, similar considerations apply. In the case of the down type quarks, the Yukawa terms can be written as [29, 30]

$$\mathcal{L}^{D}_{Yuk} = -\sum_{i=1,2,3} \sum_{j=d,s,b} Y^{D}_{ij} \bar{Q'}_{iL} \phi q'^{D}_{jR} + Y'^{D*}_{ij} \bar{q'}^{D}_{jR} \phi^{\dagger} Q'_{iL}. \tag{2.18}$$

In order to generate the Yukawa terms for u-type quarks, one has to be careful to maintain hypercharge invariance. Namely, the product $\bar{Q'}_{iL} q'^{U}_{jR}$ has hypercharge $Y = \frac{1}{2}$. Hence, with gauge invariance in mind, this bilinear should not be coupled to the Higgs which has hypercharge $Y = 1/2$, but instead one should use $\widetilde{\phi} \equiv i\sigma_2 \phi^*$, with hypercharge $Y = -\frac{1}{2}$. [5] The Yukawa terms for the u-type quarks are then given by

$$\mathcal{L}^{U}_{Yuk} = -\sum_{i=1,2,3} \sum_{j=u,c,t} Y'^{U}_{ij} \bar{Q'}_{iL} \widetilde{\phi} q'^{U}_{jR} + Y'^{U*}_{ij} \bar{q'}^{U}_{jR} \widetilde{\phi}^{\dagger} Q'_{iL}. \tag{2.19}$$

As in the previous Section, in order to find the quark mass eigenstates, we need to diagonalize the Yukawa matrices Y'^{D} and Y'^{U} by biunitary

[4] The prime symbols on top of the lepton fields denote the gauge eigenstates, *i.e.* terms that have only diagonal interactions with the gauge fields.

[5] Note that by using the Gell-Mann-Nishijima formula, this can also be seen as a consequence of the fact that the u and d quarks are contained in different components of the $SU(2)_L$ doublet Q_L [31].

transformations. Here, for the purpose of later introducing the Cabbibo-Kobayashi-Maskawa (CKM) matrix we display these transformations explicitly:

$$V_L^{D\dagger} Y'^D V_R^D = Y^D, \quad Y_{ij}^D = y_i^D \delta_{ij}, \quad i,j = d,s,b, \tag{2.20}$$

$$V_L^{U\dagger} Y'^U V_R^U = Y^U, \quad Y_{ij}^U = y_i^U \delta_{ij}, \quad i,j = u,c,t. \tag{2.21}$$

The matrices used to perform the biunitary transformations in eqs. (2.20) and (2.21) can also be used to define the mass eigenstates of quarks as follows:

$$q_L^D = V_L^{D\dagger} \begin{pmatrix} d'_L \\ s'_L \\ b'_L \end{pmatrix} = \begin{pmatrix} d_L \\ s_L \\ b_L \end{pmatrix}, \quad q_R^D = V_R^{D\dagger} \begin{pmatrix} d'_R \\ s'_R \\ b'_R \end{pmatrix} = \begin{pmatrix} d_R \\ s_R \\ b_R \end{pmatrix}, \tag{2.22}$$

$$q_L^U = V_L^{U\dagger} \begin{pmatrix} u'_L \\ c'_L \\ t'_L \end{pmatrix} = \begin{pmatrix} u_L \\ c_L \\ t_L \end{pmatrix}, \quad q_R^U = V_R^{U\dagger} \begin{pmatrix} u'_R \\ c'_R \\ t'_R \end{pmatrix} = \begin{pmatrix} u_R \\ c_R \\ t_R \end{pmatrix}, \tag{2.23}$$

where q_L^U and q_L^D refer to the first and second components of the $SU(2)_L$ doublets in flavour space respectively. After diagonalization, the quark masses are given by rescaled eigenvalues of the Yukawa matrix

$$m_i = \frac{y_i^D v}{\sqrt{2}}, \quad i = d,s,b, \tag{2.24}$$

$$m_i = \frac{y_i^U v}{\sqrt{2}}, \quad i = u,c,t. \tag{2.25}$$

The eigenvalues of the Yukawa matrices y_i^D and y_i^U are free parameters of the SM which have to be obtained from experiment.

As can be seen from the discussion above, the fermion states that have diagonal interactions with the gauge bosons do not necessarily correspond to the mass eigenstates, *i.e* states with well-defined mass. This gives rise to the quark mixing matrix known as the CKM matrix that we consider next.

In the SM two types of interactions between the fermions and bosons mediating the weak force can be distinguished. Since the currents corresponding to these interactions are coupled to charged ($W^\pm$) and neutral (Z) bosons, they are known as weak charged currents (WCC) and weak neutral currents (WNC) respectively. In this Section, the focus is on WCC, while the WNC will be considered in the next Section. The WCC originating from the covariant derivative of the lepton and quark fields is given by [29]

$$j_W^\mu = j_{W,L}^\mu + j_{W,Q}^\mu. \tag{2.26}$$

In terms of the gauge eigenstates the leptonic WCC takes the form

$$j^{\mu}_{W,L} = \sum_{i=e,\mu,\tau} \left[\bar{\nu'}_{iL}\gamma^{\mu}e'_{iL}\right]. \tag{2.27}$$

Since the neutrinos in the SM are assumed massless, one can rewrite eq. (2.27) as[6]

$$j^{\mu}_{W,L} = \overline{\boldsymbol{\nu'_L}}\gamma^{\mu}\boldsymbol{e'_L} = \overline{\boldsymbol{\nu_L}}V_L^{L\dagger}\gamma^{\mu}V_L^{L}\mathbf{e_L}, \tag{2.28}$$

where

$$\boldsymbol{\nu'_L} = \begin{pmatrix}\nu'_{eL}\\ \nu'_{\mu L}\\ \nu'_{\tau L}\end{pmatrix}, \qquad \mathbf{e'_L} = \begin{pmatrix}e'_L\\ \mu'_L\\ \tau'_L\end{pmatrix}, \tag{2.29}$$

and,

$$\boldsymbol{\nu_L} = V_L^{L}\boldsymbol{\nu'_L}, \qquad \mathbf{e_L} = V_L^{L}\mathbf{e'_L}. \tag{2.30}$$

From the unitarity of V_L^L it thus follows that

$$j^{\mu}_{W,L} = \overline{\boldsymbol{\nu_L}}\gamma^{\mu}\mathbf{e_L}. \tag{2.31}$$

Combining experimental measurements of bound QCD states with lattice calculations, it is known that all quark fields in the SM are massive. This differs from the case of leptons, where the neutrino fields are assumed massless within the context of the SM and has important consequences on the quark mixing[7] [35, 36]. The quark WCC is given by

$$j^{\mu}_{W,Q} = \sum_{i=1,2,3}\left[\overline{d'_{L,i}}\gamma^{\mu}u'_{L,i} + \overline{u'_{L,i}}\gamma^{\mu}d'_{L,i}\right]. \tag{2.32}$$

By using eqs. (2.23) and (2.22), eq. (2.32) can be written as

$$j^{\mu}_{W,Q} = \overline{\mathbf{u'_L}}\gamma^{\mu}\mathbf{d'_L} = \overline{\mathbf{u_L}}V_L^{U\dagger}\gamma^{\mu}V_L^{D}\mathbf{d_L}, \tag{2.33}$$

where the unprimed fields denote the mass eigenstates. Then the CKM matrix, defined as

$$V_q \equiv V_L^{U\dagger}V_L^{D}, \tag{2.34}$$

allows to rewrite eq. (2.33) as

$$j^{\mu}_{W,Q} = \overline{\mathbf{u_L}}V_q\gamma^{\mu}\mathbf{d_L}. \tag{2.35}$$

[6] The massless neutrino fields will remain massless after transformation by any unitary matrix. Hence the neutrino fields can be rotated by the same matrix V_L that diagonalizes the Yukawa matrix of the charged leptons.

[7] In this Section we review the original formulation of the SM, where right-handed neutrinos are not included and thus the mass term for the neutrinos is not included. In the opposite case, a mixing between neutrinos of different flavours also takes place, via the Pontecorvo-Maka-Nakagawa-Sakata (PMNS) matrix [32, 33]. For a pedagogical introduction, see [34].

Since V_q is a non-diagonal matrix, V_q thus facilitates mixing between quarks of different flavour caused by the WCC.

Now, let us investigate the form of the CKM matrix more closely. In general, a complex $N \times N$ matrix can be described by $2N^2$ values. Since V_q is unitary,[8] there are N^2 constraints on the matrix elements of V_q. Hence, V_q has N^2 independent parameters. These can be categorized into $\frac{N(N-1)}{2}$ mixing angles and $\frac{N(N+1)}{2}$ phases [29]. However, not all of the phases are observable as we will show now. For 3 generations, there are 3 mixing angles and 6 phases. The quark fields can be rephased as follows

$$q_{iL}^U \to e^{i\phi_i} q_{iL}^U, \qquad q_{jL}^D \to e^{i\phi_j} q_{jL}^D. \tag{2.36}$$

Factoring out a single phase, eq. (2.32) becomes

$$j_{W,Q}^{\mu} = +e^{-i(\psi_c - \psi_s)} \sum_{i=u,c,t} \sum_{j=d,s,b} \bar{q}_{iL}^U e^{i\psi_c - i\psi_i} \left(V_q\right)_{ij} \gamma^{\mu} q_{jL}^D e^{i\psi_j - i\psi_s}. \tag{2.37}$$

It can be easily seen from eq. (2.37) that 5 out of 6 phases in the case of $N = 3$ can be removed by rephasing the quark fields. The last phase cannot be removed, because rephasing all of the quark fields leaves the Lagrangian invariant. This is an explicit manifestation of an accidental global symmetry known as the baryon number. In summary, the CKM matrix for 3 generations of quarks has 4 parameters: 3 rotation angles and 1 phase. The elements of the CKM matrix are usually denoted as

$$V_q = \begin{pmatrix} V_{ud} & V_{us} & V_{ub} \\ V_{cd} & V_{cs} & V_{cb} \\ V_{td} & V_{ts} & V_{tb} \end{pmatrix}. \tag{2.38}$$

The standard parametrization is given by [37]

$$\begin{aligned} V_q &= \begin{pmatrix} 1 & 0 & 0 \\ 0 & c_{23} & s_{23} \\ 0 & -s_{23} & c_{23} \end{pmatrix} \begin{pmatrix} c_{13} & 0 & s_{13}e^{-i\delta} \\ 0 & 1 & 0 \\ -s_{13}e^{i\delta} & 0 & c_{13} \end{pmatrix} \begin{pmatrix} c_{12} & s_{12} & 0 \\ -s_{12} & c_{12} & 0 \\ 0 & 0 & 1 \end{pmatrix} \\ &= \begin{pmatrix} c_{12}c_{13} & s_{12}c_{13} & s_{13}e^{-i\delta} \\ -s_{12}c_{23} - c_{12}s_{23}s_{13}e^{-i\delta} & c_{12}c_{23} - s_{12}s_{23}s_{13}e^{i\delta} & s_{23}c_{13} \\ s_{12}s_{23} - c_{12}c_{23}s_{13}e^{i\delta} & -c_{12}s_{23} - s_{12}c_{23}s_{13}e^{i\delta} & c_{23}c_{13} \end{pmatrix}, \end{aligned} \tag{2.39}$$

where $s_{ij} = \sin\theta_{ij}$, $c_{ij} = \cos\theta_{ij}$ and δ is the phase responsible for the CP-violating phenomena in the flavour changing processes of the SM. All the angles θ_{ij} can be chosen inside the first quadrant, thus ensuring $s_{ij} > 0$ and $c_{ij} > 0$ [38]. Experimentally, the quark mixing angles display a well-defined hierarchy

$$s_{13} \ll s_{23} \ll s_{12} \ll 1. \tag{2.40}$$

[8] This follows directly from the definition of V_q in eq. (2.34): $V_q V_q^{\dagger} = V_L^{U\dagger} V_L^D V_L^{D\dagger} V_L^U = I$.

Fermions	g_L	g_R
ν_e, ν_μ, ν_τ	$g_L^\nu = \frac{1}{2}$	$g_R^\nu = 0$
e, μ, τ	$g_L^l = -\frac{1}{2} + s_w^2$	$g_R^l = s_w^2$
u, c, t	$g_L^U = \frac{1}{2} - \frac{2}{3}s_w^2$	$g_R^U = -\frac{2}{3}s_w^2$
d, s, b	$g_L^D = -\frac{1}{2} + \frac{1}{3}s_w^2$	$g_R^D = \frac{1}{3}s_w^2$

Table 2.2: The coefficients appearing in the neutral currents of eq. (2.45). s_w denotes the sine of the Weinberg angle defined by $g\, s_W = e$ where g is the hypercharge gauge coupling and e the unit of electric charge.

2.3 The suppression of flavour changing neutral currents

In the EW sector, the WNC can be expressed as [29]

$$j_Z^\mu = j_{Z,L}^\mu + j_{Z,Q}^\mu. \tag{2.41}$$

In terms of the gauge eigenstates, the leptonic WNC is given by

$$j_{Z,L}^\mu = \sum_{i=e,\mu,\tau} \left(2g_L^l \bar{e'}_{iL} \gamma^\mu e'_{iL} + 2g_R^l \bar{e'}_{iR} \gamma^\mu e'_{iR} \right) \tag{2.42}$$

$$+ \sum_{i=e,\mu,\tau} 2g_L^\nu \bar{\nu'}_{iL} \gamma^\mu \nu'_{iL}, \tag{2.43}$$

and the quark WNC is given by

$$j_{Z,Q}^\mu = 2 \sum_{i=u,c,t} \left(g_L^U \bar{q'}_{iL}^U \gamma^\mu q'^U_{iL} + g_R^U \bar{q'}_{iR}^U \gamma^\mu q'^U_{iR} \right) \tag{2.44}$$

$$+2 \sum_{i=d,s,b} \left(g_L^D \bar{q'}_{iL}^D \gamma^\mu q'^D_{iL} + g_R^D \bar{q'}_{iR}^D \gamma^\mu q'^D_{iR} \right). \tag{2.45}$$

The coefficients $g_L^{U,D}$ are shown in Table 2.2.

Given that the mass eigenstates of quarks are not aligned with the gauge eigenstates, it is interesting to investigate whether the transformation between these states changes the mathematical form of the WNC. To that end, the matrices V^D and V^U introduced in the previous Section along with eqs. (2.23) and (2.22) can be used to transform the quark neutral currents

from the diagonal gauge eigenstate basis into the mass basis:

$$\begin{aligned} j^{\mu}_{Z,Q} &= 2g^{U}_{L}\bar{\mathbf{q}}^{\mathbf{U}}_{\mathbf{L}}V^{U}_{L}\gamma^{\mu}V^{U\dagger}_{L}\mathbf{q}^{\mathbf{U}}_{\mathbf{L}} + 2g^{U}_{R}\bar{\mathbf{q}}^{\mathbf{U}}_{\mathbf{R}}V^{U}_{R}\gamma^{\mu}V^{U\dagger}_{R}\mathbf{q}^{\mathbf{U}}_{\mathbf{R}} \\ &+ 2g^{D}_{L}\bar{\mathbf{q}}^{\mathbf{D}}_{\mathbf{L}}V^{D}_{L}\gamma^{\mu}V^{D\dagger}_{L}\mathbf{q}^{\mathbf{D}}_{\mathbf{L}} + 2g^{D}_{R}\bar{\mathbf{q}}^{\mathbf{D}}_{\mathbf{R}}V^{D}_{R}\gamma^{\mu}V^{D\dagger}_{R}\mathbf{q}^{\mathbf{D}}_{\mathbf{R}} \\ &= 2g^{U}_{L}\bar{\mathbf{q}}^{\mathbf{U}}_{\mathbf{L}}\gamma^{\mu}\mathbf{q}^{\mathbf{U}}_{\mathbf{L}} + 2g^{U}_{R}\bar{\mathbf{q}}^{\mathbf{U}}_{\mathbf{R}}\gamma^{\mu}\mathbf{q}^{\mathbf{U}}_{\mathbf{R}} \\ &+ 2g^{D}_{L}\bar{\mathbf{q}}^{\mathbf{D}}_{\mathbf{L}}\gamma^{\mu}\mathbf{q}^{\mathbf{D}}_{\mathbf{L}} + 2g^{D}_{R}\bar{\mathbf{q}}^{\mathbf{D}}_{\mathbf{R}}\gamma^{\mu}\mathbf{q}^{\mathbf{D}}_{\mathbf{R}}. \end{aligned} \tag{2.46}$$

Evidently, the unitarity of the transformation matrices $V^{U}_{L,R}$ and $V^{D}_{L,R}$ guarantees that there are no tree level flavour changing neutral currents (FCNCs) in the quark sector of the SM. Using similar arguments, it can also be shown that at the loop level, the FCNC-s are suppressed due to the unitarity of the CKM matrix. This is known as the GlashowIliopoulosMaiani (GIM) mechanism [13]. Analogously, the same result also holds true for leptonic FCNC. As we will see in Chapter 5 the GIM mechanism in the SM gives an important handle on NP beyond the SM whereby significant contributions to FCNC-s may occur.

2.4 The flavour hierarchy problem in the Standard Model

The numerical values of the fermion masses obtained from experimental observations and lattice calculations exhibit a large hierarchy of the extent of many orders of magnitude [39]. This hierarchy is displayed in Fig. 2.1. In the context of the SM the hierarchy in fermion masses is ascribed to the hierarchy of the Yukawa couplings that are controlling the size of the masses after the SSB. Crucially, however, the SM does not attempt to explain the spread in the Yukawa couplings which are only added into the SM as free parameters fixed by experiment.

Analogously to the fermion masses, the CKM matrix elements also exhibit a noticeable hierarchy. This is depicted in Fig. 2.2. Similarly, to the fermion masses, the hierarchy of the CKM elements can be ascribed to the hierarchy of the Yukawa couplings. The hierarchy of the CKM elements and the fermion masses together constitute the flavour hierarchy problem, whereby highly specific *a priori* unmotivated choice of model inputs is needed to explain the hierarchy of experimentally observed quantities. Instead, it would be more satisfactory to have a construction whereby the hierarchy is dynamically generated from model inputs all of the same order of magnitude. This can be achieved in many extensions of the SM, wherein the hierarchy in Yukawa couplings is generated via BSM interactions involving new fields and symmetries [42–50].

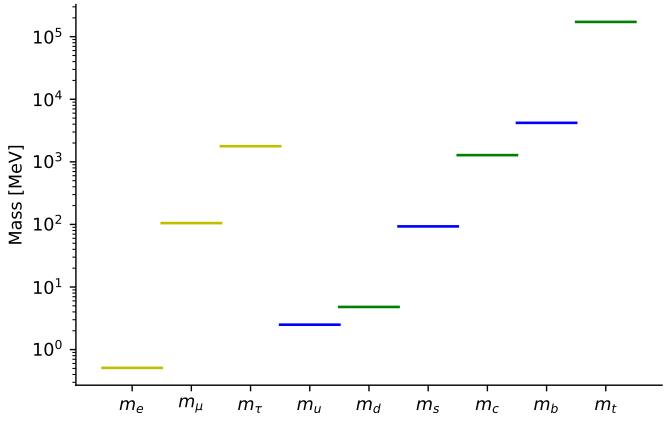

Figure 2.1: The order of magnitude hierarchy of the charged fermion masses in the SM. The yellow lines depict the masses of the charged leptons, the blue lines the masses of the u-type quarks and the green lines the masses of the d-type quarks. The upper bound for the neutrino masses is known to be at sub-eV scales due to constraints from cosmology. However, since the absolute scale for the neutrino masses is unknown, the individual values are not shown on this plot. Figure taken from the Master's Thesis of the dissertant [40].

.

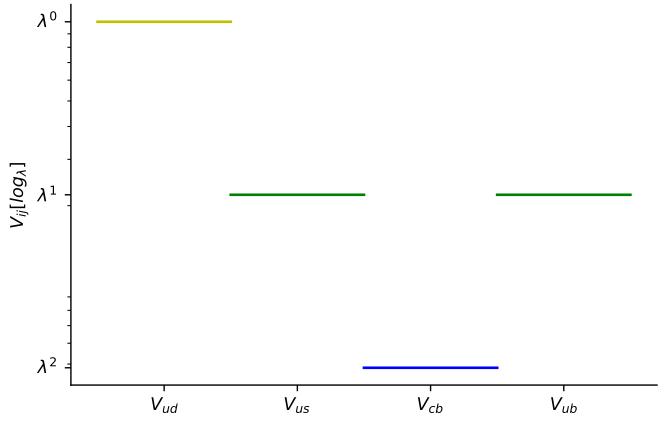

Figure 2.2: The hierarchy of the 4 independent physical parameters of the CKM matrix. The chosen matrix elements of V_q can be fitted as powers of the Cabibbo angle $\lambda \approx 0.22$ [41]. In particular, the elements span 3 orders of magnitude. Figure taken from the Master's Thesis of the dissertant [40].

Chapter 3

The electroweak vacuum stability

As was shown in the previous Section, the masses of the elementary fermions of the SM are proportional to the value of the Higgs vev. In addition, though not shown explicitly in this Thesis, the same conclusion also holds for the masses of the Higgs boson, the gauge bosons and the interactions of all SM particles with the Higgs boson. Thus the Higgs vev is a unique energy scale that governs the masses of all the SM particles. Experimentally, the Higgs vev v is fixed by the measurement of the Fermi coupling G_F through the following relation

$$v = \frac{1}{\sqrt{\sqrt{2}G_F}}, \tag{3.1}$$

wherein G_F has been determined to the accuracy of 0.6 parts per million using muon decay measurements [39]. This fixes $v = 246$ GeV. This particular expectation value of the Higgs field at tree level is what we will call the Higgs vev from now on.[1] However, the Higgs vev may not correspond to the global minimum of the Higgs potential due to quantum corrections arising from loop diagrams which can destabilize the potential by introducing a deeper minimum at larger field values. The modifications to Higgs potential by higher order corrections have been comprehensively studied after the discovery of the Higgs boson and it has been established that the SM vacuum develops another, deeper minimum at $h \simeq 10^{10}$ GeV [18, 51, 52]. The global minimum of the Higgs potential at higher field values does not necessarily pose a cosmological problem as long as the lifetime of the false vacuum associated with the Higgs vev is longer than the current age of the Universe [53]. Through a careful, next-to-next-to-leading order (NLLO)

[1] This distinction is necessary since the Higgs potential can also admit other vacua with different expectation values for the Higgs field due to quantum corrections to the Higgs potential.

analysis of the Higgs potential, it has been shown that this is indeed the case for the measured values of top quark and Higgs boson masses in the SM, rendering the false vacuum metastable [18].

Nevertheless, for metastable vacua, an exponentially suppressed probability of tunneling from the false vacuum to the true vacuum remains. Moreover, the metastability of the Higgs vacuum depends quite strongly on the value of the top quark mass, with the EW vacuum becoming unstable for $m_t > 177$ GeV once the Higgs boson mass is fixed at $m_h = 125$ GeV [18].

Instead, if one considers models of NP, including new fields and symmetries beyond the SM, the EW vacuum corresponding to $v = 246$ GeV can be rendered stable even for the observed values of the Higgs boson and top quark masses [54, 55].

3.1 The effective potential of the SM

To show how quantum corrections may alter Higgs vacuum stability, we begin by first considering the 1-loop Higgs effective potential of the SM. In this Section, we are closely following the excellent review of effective potentials offered in [56].

In the presence of an external source J, one can define the partition function $Z[J]$, which describes the amplitude of the transition between two vacuum states at asymptotic times ($t \to \pm\infty$) corresponding to the states with minimal energy $|\Omega\rangle$:

$$\langle\Omega|\Omega\rangle_J = Z[J] = \int \mathrm{D}h e^{\frac{i}{\hbar}\left(S[h]+\int d^4x J(x)\, h(x)\right)} = e^{\frac{i}{\hbar}W[J]}, \tag{3.2}$$

where $S[h] = \int d^4x \mathcal{L}[h(x)]$ and we have defined another functional $W[J]$ that is known as the generating functional. Next, we define the classical background field $\hat{h}$ as the expectation value of h in the presence of J. This can be understood as the average of all the possible fluctuations around the vacuum. In more detail,

$$\hat{h}(x) = \langle\Omega|\, h(x)\, |\Omega\rangle_J = \frac{1}{Z[J]} \int \mathrm{D}h\, h(x)\, e^{\frac{i}{\hbar}\left(S[h]+\int d^4x J(x)h(x)\right)} = \frac{\delta W[J]}{\delta J(x)}. \tag{3.3}$$

Note that for $J = 0$, eq. (3.3) describes the expectation value of h in the true vacuum of the theory. It is clear from eq. (3.3) that $\hat{h}$ is a conjugate variable to $J(x)$. Hence we can define the Legendre transform of $W[J]$

$$\Gamma[\hat{h}] = W[J] - \int d^4x J(x)\hat{h}(x). \tag{3.4}$$

$\Gamma[\hat{h}]$ is known as the effective action and it is given by the sum of 1-particle irreducible (1PI) graphs. From the definition of $\Gamma[\hat{h}]$ it immediately follows that

$$\frac{\delta\Gamma[\hat{h}]}{\delta\hat{h}} = -J(x) \implies \left.\frac{\delta\Gamma[\hat{h}]}{\delta\hat{h}}\right|_{J=0} = 0. \tag{3.5}$$

Thus we already notice that in the absence of external sources, the classical field corresponds to the configuration minimizing the effective action. To proceed, we notice that $\Gamma[\hat{h}]$ can also be expanded in series

$$\Gamma[\hat{h}] = -\int d^4x V_{\text{eff}}[\hat{h}] + \int d^4x \frac{1}{2} Z[\hat{h}] \left(\partial_\mu \hat{h}\right)^2 + ..., \tag{3.6}$$

where the dots denote higher order terms in powers of $\partial_\mu \hat{h}$ and $V_{\text{eff}}[\hat{h}]$ and $Z[\hat{h}]$ correspond to the coefficients of the expansion. Then, assuming that the classical background field is homogenous, we obtain in the absence of sources[2]

$$\left.\frac{\partial V_{\text{eff}}(\hat{h})}{\partial\hat{h}}\right|_{\hat{h}_0} = 0. \tag{3.7}$$

Recalling the discussion above, we can then conclude that the expectation value of the field h in the absence of external sources, *i.e.* the true vacuum of the theory corresponds to the minimum of the V_{eff}. For this reason, V_{eff} is known as the effective potential. Thus, to find the effect of the quantum corrections on the true vacuum of the theory, one can just compute the loop corrections to V_{eff} and minimize the potential to find the ground state.

There are several ways in which the effective potential, including the loop corrections can be computed. An elegant method, employing the path integral formalism was put forward by Jackiw [58]. His approach can be summarized in the following simple steps.

1. Start from eq. (3.2), and decompose it as follows: $h \to \hat{h} + h_q$, where $\hat{h}$ is the classical background field appearing in the discussion above and h_q is a quantum field satisfying $\langle h_q \rangle = 0$, where the expectation value of h_q is defined in the same way as for h in eq. (3.3).

2. Respecting the condition $\langle h_q \rangle = 0$, drop all the terms linear in h_q from the Lagrangian.

[2]This assumption is not always justified. For instance, when a discrete symmetry is spontaneously broken, domain walls may form where the background field takes different values in different causally disconnected patches in the Universe [57]. However, for our purposes, this issue is not relevant as in our proposed NP model there are no domain walls.

i	$W^{\pm}$	Z	h	G_0	$G^{\pm}$	t
n_i	6	3	1	1	2	-12
C_i	$\frac{5}{6}$	$\frac{5}{6}$	$\frac{3}{2}$	$\frac{3}{2}$	$\frac{3}{2}$	$\frac{3}{2}$

Table 3.1: The values of C_i and n_i appearing in eq. (3.8) assuming the choice of the $\overline{\text{MS}}$ renormalization scheme.

3. The effective potential is then given by the sum of the vacuum graphs of the theory.

For the SM at 1-loop the prescription presented above yields the following form the effective potential [59] [3]

$$V_{\text{eff}}(\hat{h}) = -\frac{\mu^2}{2}\hat{h}^2 + \frac{\lambda_H}{4}\hat{h}^4 + \frac{1}{64\pi^2}\sum_i n_i m_i^4(\hat{h})\left[\ln\frac{m_i^2(\hat{h})}{\mu^2} - C_i\right], \quad (3.8)$$

with $i \in \{W^{\pm}, Z, h, G_0, G^{\pm}, t\}$, where G^0 and $G^{\pm}$ denote the Goldstone bosons associated with the 3 unphysical components of the Higgs doublet ϕ introduced in Chapter 2. [4] The renormalization scale μ is an arbitrary energy scale that should be chosen in such a way as to ensure that perturbativity holds, as will be discussed in the next Section. The constants n_i encode the degrees of freedom of the associated particles and C_i are constants inherent to the chosen renormalization scheme. The values of n_i and C_i for all the relevant particles are summarized in Table 3.1. Note that due to the hierarchy of the Yukawa couplings of the SM fermions, only the contribution of the top Yukawa coupling has a sizeable effect on the SM effective potential and thus the contribution of the other fermions of the SM has been omitted from eq. (3.8).

The field-dependent masses m_i are defined as the second derivatives of the potential with respect to the field under consideration. Specifically, one has for scalars

$$m_h^2(\hat{h}) = \left.\frac{\partial^2 V}{\partial h^2}\right|_{h=\hat{h}} = -\mu_H^2 + 3\lambda_H\hat{h}^2, \quad (3.9)$$

and

$$m_{G_0}^2(\hat{h}) = m_{G^{\pm}}^2(\hat{h}) = \left.\frac{\partial^2 V}{\partial G_0^2}\right|_{h=\hat{h}} = -\mu_H^2 + \lambda_H\hat{h}^2. \quad (3.10)$$

[3] Here we use the Landau gauge in order to avoid the appearance of ghosts and the $\overline{\text{MS}}$ renormalization scheme.

[4] The unphysical Goldstone bosons appear here due to our choice of gauge. In the unitarity gauge these contributions do not appear.

Similarly, field-dependent masses of the gauge bosons and the top quark are given by

$$m_{W^\pm}^2(\hat{h}) = \frac{g^2}{4}\hat{h}^2, \quad m_Z^2(\hat{h}) = \frac{g'^2 + g^2}{4}\hat{h}^2, \quad m_t^2(\hat{h}) = \frac{y_t^2}{2}\hat{h}^2, \tag{3.11}$$

where y_t is the largest eigenvalue of the Yukawa matrix for the up quarks. Looking at eq. (3.8) we notice the presence of one logarithmic contribution to the effective potential with a negative sign, namely the one associated to the top quark. Thus for large enough y_t the potential can be unbounded from below at large field values, signaling that the EW vacuum is unstable. Alternatively, for specific values of λ_H and y_t there can also be another minimum at $h_{\min} \gg 246$ GeV with the potential again increasing for $h > h_{\min}$. In this case, the EW vacuum is said to be metastable.

As was mentioned before, for the measured values of the SM parameters, it turns out that the EW vacuum is metastable with another vacuum appearing at $h_{min} \simeq 10^{10}$ GeV. However, this conclusion might be altered by NP effects which change the functional form of the effective potential due to the new fields and interactions. However, before examining the effects of NP on vacuum stability we need to take care of a subtlety related to the perturbativity of the effective potential.

3.2 Renormalization group improvement of the effective potential

In eq. (3.8) we presented the effective potential up to 1-loop contributions. It can be shown that higher loop contributions introduce higher powers of the logarithms appearing in eq. (3.8) [60]. In more detail, if we denote the couplings multiplying the logarithms in eq. (3.8) collectively by λ, and the logarithm by L the structure of the 1-loop corrections to the tree level potential (denoted by $V_{\text{1-loop}}$) can schematically be written as

$$V_{\text{1-loop}} \sim \lambda L + \lambda. \tag{3.12}$$

At two loops higher powers of the logarithm also appear. Explicitly, we have [56]

$$V_{\text{2-loop}} \sim \lambda^2 L^2 + \lambda^2 L + \lambda^2. \tag{3.13}$$

Generalizing to N-loop corrections, we then have

$$V_{\text{N-loop}} \sim \lambda^N L^N + \lambda^N L^{N-1} + \lambda^N L^{N-2} + ... + \lambda^N. \tag{3.14}$$

Formally, the first term in eq. (3.14) is called the leading log (LL), the second one is called the next-to-leading log (NL), the third one the next-to-next-to leading log (NLL) and so on. From this observation, it is clear

that higher loop corrections can only be neglected if the following conditions are satisfied

$$\lambda \lesssim 1 \quad \text{and} \quad L \lesssim 1. \tag{3.15}$$

In particular, not only should the couplings of the theory be small, but the logarithms should also be kept small in order for the perturbative expansion to hold. Specifically, the second condition of eq. (3.15) may not be satisfied if one naively fixes the renormalization scale μ at a constant value. To illustrate this point, suppose we fix $\mu = v$, where v denotes the Higgs vev. Then, for coupling constants of the order 10^{-1}, $L \gtrsim 1$ for already $h \gtrsim 10^5$ GeV, while the loop corrected SM potential develops a global minimum at much higher field values.

However, in all of the discussion above we have neglected a crucial feature of renormalization. Namely, the scale μ appearing in all of the logarithms of eq. (3.14) is an arbitrary energy scale introduced via the process of dimensional regularization. Since the effective potential is a physical observable, its value should not depend on this scale. Thus, we get the following equality

$$\frac{d\, V_{\text{eff}}(\hat{h})}{d\mu} = 0. \tag{3.16}$$

Using chain rule, eq. (3.16) becomes

$$\left(\mu\frac{\partial}{\partial\mu} + \beta_{g_i}\frac{\partial}{\partial g_i} + \mu_H^2\beta_{\mu_H}\frac{\partial}{\partial\mu_H^2} + \gamma\hat{h}\frac{\partial}{\partial\hat{h}}\right) V_{\text{eff}} = 0, \tag{3.17}$$

where $g_i = g', g, g_s, \lambda_H, y_t$ and the coefficients

$$\beta_{g_i} = \mu\frac{dg_i}{d\mu}, \quad \beta_{\mu_H} = \frac{\mu}{\mu_H^2}\frac{\partial\mu_H^2}{\partial\mu}, \tag{3.18}$$

and

$$\gamma = \frac{\mu}{\hat{h}}\frac{d\hat{h}}{d\mu}, \tag{3.19}$$

are known as the beta functions and anomalous dimensions, respectively. Solving this equation, known as the Callan-Symanzik equation, [61–63] we can formally find the effective potential to all orders. The exact solution to the Callan-Symanzik equation was derived in [64] via the method of characteristics. The result is given by

$$V_{\text{eff}}(\hat{h}) = \frac{1}{2}\mu_H^2 G^2(t)\hat{h}^2 + \frac{1}{4}\lambda_H(t)G^4(t)\hat{h}^4, \tag{3.20}$$

with

$$t = \log\frac{\hat{h}}{\mu} \quad \text{and} \quad G(t) = e^{-\int_0^t dt'\frac{\gamma}{1-\gamma}}, \tag{3.21}$$

and the Higgs mass term and the coupling constants satisfying

$$\frac{dg_i}{dt} = \frac{\beta_{g_i}}{1-\gamma}, \qquad \frac{d\mu_H^2}{dt} = \mu_H^2 \frac{\beta_{\mu_H}}{1-\gamma}. \tag{3.22}$$

We notice that the explicit scale dependence in the logarithms of the effective potential is compensated by the implicit scale dependence due to the *running* of the couplings g_i as functions of the energy scale μ. Indeed, the combination of these two effects ensures that the Callan-Symanzik equation is satisfied order-by-order and the effective potential is scale-independent.

Eq. (3.20) is an exact solution to the Callan-Symanzik equation that holds up to all orders of perturbation theory, provided one is able to compute the β-functions and the anomalous dimensions exactly [65]. In practice however, these quantities can only be computed up to finite numbers of loops and so eq. (3.20) represents an approximation to the exact effective potential that becomes more accurate with the addition of higher order loop corrections to the β-functions and anomalous dimensions. In terms of re-summing the large logarithms, it has been shown that using 1-loop corrections to calculate the $\mu^2(t), \lambda(t), G(t)$ re-sums the LL contributions, the 2-loop corrections re-sums the NLL contributions and so on.

3.3 The electroweak vacuum stability in the SM

Anticipating that loop corrections usually generate additional minimum to the Higgs potential at much higher field values than the Higgs vev, we can neglect the first term in eq. (3.20). Moreover, for the 1- and 2-loop computations that we are interested in the effect of γ is typically very small and thus we can safely set $\gamma \approx 0$, $G(t) \approx 1$. As a result, we can approximate the effective potential of the SM at large field values as [5]

$$V_{\text{eff}}(h) \approx \frac{\lambda_H(t)}{4} h^4. \tag{3.23}$$

Then, the minima of the potential are solely determined by the running of $\lambda_H(t)$ at large field values, *i.e.* when $t >> 1$. More precisely, there are three different options[6]:

[5] Since in this discussion, it is clear that we always consider the classical background field value of the quantum field h, we drop the "hat" symbol from all expressions involving h from now on.

[6] In all of these cases covered in this Chapter, we only consider running until the Planck scale, at which the onset of NP effects associated with quantum gravity is expected to modify the simple analysis presented here. In more general theories such as for instance [44] Landau poles may be encountered at scales lower than the Planck scale. In this case, the stability of the potential should only be examined up to the scale at which the Landau pole appears.

1. λ_H never runs negative at large field values. In that case the potential is always increasing and there is no other minimum besides the EW minimum.

2. If λ becomes negative at t satisfying $t_1 < t < t_2$ and then becomes positive again for all $t > t_2$, then the potential develops a new global minimum at $h \gg v$, i.e the EW vacuum becomes metastable.

3. If there exists a t_* such that $\lambda_H(t)$ is negative for all $t > t_*$ then the potential has no absolute minimum, and the EW vacuum is said to be unstable.

3.4 Vacuum stability in the SM

To gain more insight into the vacuum stability of the SM, let us focus on a simple scenario using eq. (3.23) and the running of λ at two loops. This allows us to study the effective potential up to NLL accuracy. It is important to remark, that in the present analysis, we neglect threshold corrections, associated with the decoupling of heavy physics at low energies (for more details see [18]), so our analysis only provides a qualitative picture of how the instability may set in. However, the scale of the instability predicted by our simple analysis is in fact of the same order of magnitude as the value found in [18].

The running of the Higgs quartic coupling λ_H at two loops is depicted on Fig. 3.1 which summarizes the running from the top mass scale $m_t = 173$ GeV up to the scale of the reduced Planck mass $M_{Pl} = \frac{1.22}{\sqrt{8\pi}} \times 10^{19}$ GeV. It can be seen that the effective potential in the approximation of eq. (3.23) is stable until $h = 10^{10}$ GeV, at which point the quartic coupling λ_H starts to obtain negative values and the potential is unbounded from below. For $h > 10^{12}$ GeV, the quartic coupling plateaus to a constant value. At these values, the effective potential is still unbounded below and can be approximated as

$$\lambda(h \gtrsim 10^{12}\ \text{GeV}) \simeq \frac{\lambda(h = 10^{12}\ \text{GeV})}{4} h^4. \tag{3.24}$$

The scale-dependence of the gauge couplings and the top Yukawa couplings responsible for the running of λ_H is displayed on Fig. 3.2. It can be deduced that λ_H flows rapidly toward zero at small field values when the top Yukawa coupling and the strong gauge coupling dominate. In fact, from the form of the two loop β-function for λ_H it can be seen that the only negative contribution of g_s depends on the product of g_s and y_t, so it is maximized when

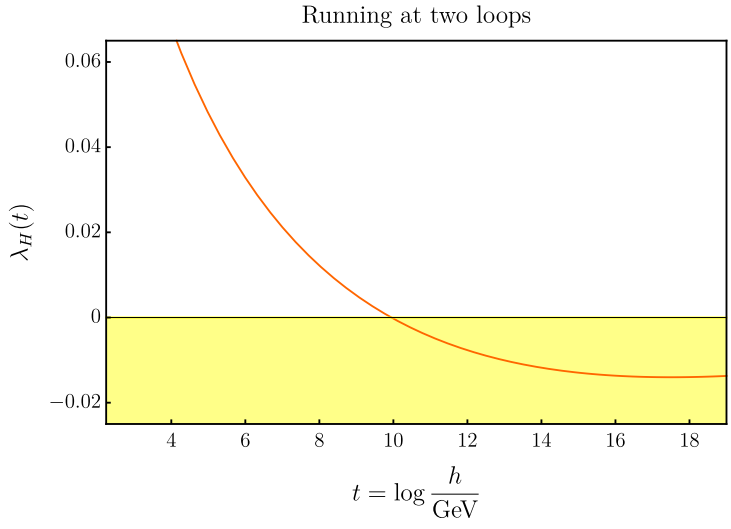

Figure 3.1: Running of $\lambda_H(t)$ as a function of t at two loops. The yellow region represents the range of λ_H where the potential is unstable.

both g_s and y_t are large. [7] Hence, y_t can be regarded as the most important coupling governing vacuum stability. Once the top Yukawa coupling becomes smaller than the normalized hypercharge coupling g_1, λ_H runs negative after which λ_H plateaus to a constant value. This occurs both due to the decreasing effect of the top Yukawa and the strong gauge coupling as a function of increasing energy and because the terms in β_{λ_H} containing odd powers of λ_H that drove λ_H to negative values when $\lambda_H > 0$ will have the opposite effect when $\lambda_H < 0$.

3.5 Electroweak vacuum stability in extensions of the SM

From the previous discussion we learned that the instability of the Higgs potential is mainly driven by the sizeable top Yukawa coupling. Consequently, one might wonder if vacuum stability could be achieved in NP models where the Yukawa couplings between the SM fermions and the Higgs boson are forbidden in the Lagrangian. In this case, the Yukawa terms of the SM fermions could be generated via higher-order operators involving the interaction of the Higgs boson with new BSM fields.[8] Thus, above the scale

[7] Here, for the sake of brevity, we do not display the 2-loop β-functions for the coupling. For reference, the β-functions can be found from [66].

[8] Examples of models along these lines can be found for instance from [42, 43, 67].

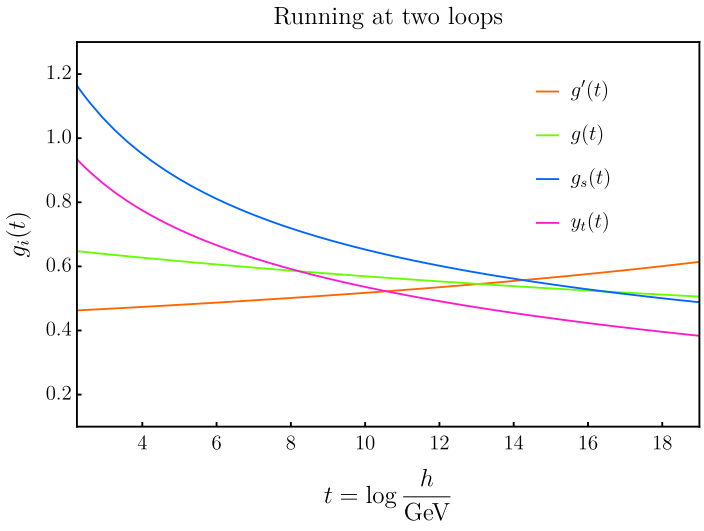

Figure 3.2: Running of the other couplings $g_i(t)$ that drive the running of $\lambda_H(t)$. Notice that for convenience we use the grand unified theory normalization to define $g_1 = \sqrt{\frac{5}{3}}g'$.

of the effective operators, the SM Yukawa terms do not contribute to the running of λ_H but instead, the contribution from the interaction between the new fields and the Higgs boson should be added.

Forasmuch as the new interactions can also drive the Higgs quartic to negative values, the condition that SM Yukawa terms are forbidden in the Lagrangian is by itself not enough to ensure vacuum stability. In particular, instability often arises when the new interactions are fermionic since the sizeable Yukawa couplings between the Higgs boson and the new fermions again drive λ_H to negative values similar to the case of the top Yukawa in the SM. A clear example of this situation is provided by the models that explain the fermion masses through the universal seesaw mechanism [68–71].

On the contrary in models where the SM Yukawa couplings are generated via the interaction of the Higgs boson with new, bosonic degrees of freedom, vacuum stability is instead not threatened by the interaction of the Higgs boson with the new fields. The generated top Yukawa then takes the form

$$\frac{c_t}{\Lambda} h\bar{t}t, \tag{3.25}$$

where c_t represents the corresponding Wilson coefficient and Λ is a cut-off scale of the order of the mass of the heavy particles interacting with the Higgs field [42,43,67]. Above the scale Λ the Yukawa interaction for the top

quark (t) ceases to be a local operator and thus does not contribute to the running of λ_H [44]. It is then clear, that vacuum stability can be achieved as long as $\Lambda < h_*$ where h_* corresponds to the SM instability scale which in the previous Section was shown to be $h_* \simeq 10^{10}$ GeV.

Chapter 4

Muon anomalous magnetic moment

Given the rich particle content of the SM, it is natural to ponder whether there can be any other light particles below or around the EW scale. Even though with the current collider experiments running up to the center of mass energies of 14 TeV, many hypotheses of light physics below the TeV scale have been heavily constrained, this possibility has not yet been ruled out completely. One particular way in which effects of light NP can appear is through loop contributions to observables that are measured up to very high accuracy. To that end, it is customary to use the magnetic moments of leptons whose measurements constitute some of the most accurate experiments ever made in physics.

At the classical level, the magnetic moment $\vec{\mu}_L$ is formed when a charged particle is spinning with angular momentum $\vec{L}$

$$\vec{\mu}_L = \frac{e}{2m}\vec{L}, \qquad \text{with} \qquad \vec{L} = m\vec{r} \times \vec{v}. \tag{4.1}$$

The magnetic moment of a spinning particle, $\vec{\mu}_L$, is influenced by the presence of an external magnetic $\vec{B}$. In particular, looking at the corresponding Hamiltonian,

$$\mathcal{H} = -\vec{\mu}_L \cdot \vec{B}, \tag{4.2}$$

we see that the external field $\vec{B}$ has the effect of rotating μ_L in its direction, thus minimizing the energy of the system.

At the quantum level, the charged elementary fermions cannot be considered as spinning particles, yet they still possess *intrinsic* angular momentum that cannot be visualized as being associated with classical motion, but should instead by identified with an inherent property of these particles, called the spin of the fermion. The spin operator $\vec{S}$ is given by

$$\vec{S} = \frac{\vec{\sigma}}{2}, \tag{4.3}$$

where $\vec{\sigma}$ denotes the Pauli sigma matrices. For an elementary lepton of charge e, the magnetic moment generated by its spin is then given by

$$\hat{\vec{\mu}}_L = gQ\frac{e}{2m}\frac{\vec{\sigma}}{2}, \tag{4.4}$$

where g is a dimensionless number, called the gyromagnetic ratio, $Q = 1$ for leptons and $Q = -1$ for antileptons, e is the unit elementary charge and m is the mass of the particle.

To a first approximation, the value of g_s in a quantum theory can be inferred by looking at the non-relativistic limit for the lepton wavefunction ϕ:

$$i\hbar\frac{\partial\phi}{\partial t} = \left[\frac{\vec{p}^2}{2m} - \frac{e}{2m}(\vec{L} + 2\vec{S})\cdot\vec{B}\right]\phi, \tag{4.5}$$

where $\vec{p}$ denotes the momentum operator, $\hbar$ is the reduced Planck constant, and $\vec{L}$ and $\vec{S}$ denote the orbital angular momentum and the spin angular momentum of the lepton respectively. Comparing eqs. (4.4) and (4.5) it appears that to a first approximation, ignoring higher loop corrections $g = 2$ as predicted first by P. Dirac in 1928 [72].

However, this result does not take into account loop corrections, which may have non-negligible effects on the value of g. This deviation is usually defined in the following way

$$a = \frac{1}{2}(g - 2), \tag{4.6}$$

and is known as $g-2$ or the anomalous magnetic moment. In what follows, we will explain how loop corrections result in non-zero values of a and why the muon is the most suitable particle to measure this deviation.

In relativistic quantum electrodynamics (QED) the anomalous magnetic moment can be extracted from the form factor in the matrix element $\mathcal{M}$ describing the scattering of a lepton in an external electric field:

$$\mathcal{M} = \left\langle l(p')\right| j_{EM}(0)\left|l(p)\right\rangle, \tag{4.7}$$

where p and p' denote the 4-momentum before and after scattering, respectively and the electromagnetic current j_{EM} corresponding to the external electromagnetic field has been evaluated at zero momentum transfer in concordance with the classical limit. The Feynman-diagrammatic representation of this interaction is displayed in Fig. 4.1. The corresponding matrix element can be decomposed as

$$\mathcal{M} = (-ie)\bar{u}(p')\left[\gamma^\mu F_E(q^2) + i\frac{\sigma^{\mu\nu}}{2m_l}F_M(q^2)\right]u(p), \tag{4.8}$$

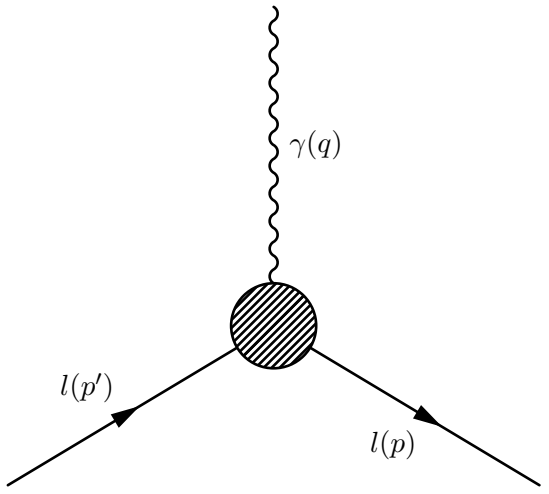

Figure 4.1: Feynman diagram contributing to g-2 of an lepton l. The blob depicts the form factor which is modified by loop corrections.

where m_l is the mass of the corresponding lepton, $\bar{u}, u$ are the Weyl spinors resulting from the plane wave expansion of the Dirac spinor l and $F_E(q^2)$ and $F_m(q^2)$ are the electric and magnetic form factors which depend on the squared 4-momentum q of the photon. The operator $\sigma_{\mu\nu}$ is defined by

$$\sigma^{\mu\nu} = \frac{i}{2}\left[\gamma^\mu, \gamma^\nu\right]. \tag{4.9}$$

As mentioned before, in the classical limit $q^2 = 0$, and in that case, the form factors obey the following equations:

$$F_E(0) = 1, \tag{4.10}$$

and

$$F_M(0) = a. \tag{4.11}$$

The first of these equations is governed by the renormalization of electric charge, while the second one defines the anomalous magnetic moment introduced by eq. (4.4).

In 1948 Schwinger, calculated a to 1-loop level, including only QED corrections. He obtained [73]

$$a^{\mathrm{QED}} = \frac{\alpha}{2}, \tag{4.12}$$

with $\alpha = \frac{e^2}{4\pi}$ denoting the fine-structure constant of electromagnetism. Eq. (4.12) is modified by higher-order corrections including also the effects

of the strong and weak interactions, and possible effects of NP. A detailed description of corrections to a at different loop orders can be found in [74]. At higher loop orders the form factors evaluated at $q^2 = 0$ are generally complex numbers. Hence it is often customary to define the effective dipole moment D via:

$$\mathcal{L}_{\text{eff}}^{\text{dipole}} = -\frac{1}{2}\left[\bar{l}\sigma^{\mu\nu}\left(D\frac{1+\gamma_5}{2} + D^*\frac{1-\gamma_5}{2}\right)l\right]F^{\mu\nu}, \tag{4.13}$$

where $F^{\mu\nu} = \partial^\mu A^\nu - \partial^\nu A^\mu$. The real and imaginary components of D can then be identified with the magnetic and electric dipole moments respectively:

$$\text{Re}\, D = a\frac{e}{2m_l}, \quad \text{Im}\, D = \frac{\eta}{2}\frac{e}{2m_l}, \tag{4.14}$$

where η is defined in analogy to g, namely via relating the electric dipole moment $\vec{d}$ of the charged lepton to the Pauli spin matrices as follows:

$$\vec{d} = \eta\, Q\, \mu_0 \frac{\vec{\sigma}}{2}. \tag{4.15}$$

This particular dependence of the dipole moments D is a reflection of the fact that the magnetic dipole moment interactions are charge-parity (CP) -conserving, while the electric dipole moment interactions violate the CP symmetry [74]. Thus the measurement of electric dipole moments provides a handle for constraining models featuring CP-violation. In the SM the electric dipole moments of the elementary leptons are highly suppressed due to the hierarchical structure of the Yukawa couplings described in Chapter 2. The measured values for the electron and muon dipole moments are

$$d_e < 0.87 \times 10^{-28}\text{e} \cdot cm, \qquad d_\mu < 1.8 \times 10^{-19}\text{e} \cdot cm. \tag{4.16}$$

Looking at eq. (4.13) it is clear that the Lagrangian term giving rise to the dipole moments is of dimension 5. Thus in a renormalizable theory, dipole moments are calculable quantities that cannot be chosen as input parameters. This, along with the fact that the dipole moments can be measured with extremely good accuracy makes them very useful observables for investigating possible models of NP.

To understand why it is useful to consider the muon magnetic dipole moment in particular, let us note that the loop corrections to the dipole moments can be estimated as [74]

$$\delta a \simeq \frac{m_l^2}{M^2}, \tag{4.17}$$

where M corresponds to particles with mass scales above m_l. Since the muon is approximately 10^2 times heavier than the electron, we see that the

sensitivity of the anomalous magnetic moment of muon is enhanced by a factor of 10^4 compared to that of the electron. The enhancement would be even stronger for the τ-lepton which is heavier than the muon by a factor of 10. However, due to the small lifetime of τ its magnetic moment cannot be measured accurately enough to be used as a probe of NP. Eq. (4.17) also clearly shows that the magnetic moments are sensitive to light NP since the effects of heavy physics are suppressed by the heavy mass in the denominator.

In 2021, the Muon $g-2$ collaboration at Fermilab released [75, 76] the new measurement of the anomalous magnetic moment of the muon, $a_\mu = \frac{1}{2}(g-2)_\mu$. The result of the previous Brookhaven E821 muon $g-2$ experiment was [77] $a_\mu^{\rm E821} = 116592089(63) \times 10^{-11}$, and had a deviation of about 3.7σ, $\Delta a_\mu^{\rm E821} = a_\mu^{\rm E821} - a_\mu^{\rm SM} = (279 \pm 76) \times 10^{-11}$ compared with the SM contribution [78]

$$a_\mu^{\rm SM} = (116591810 \pm 43) \times 10^{-11}. \tag{4.18}$$

The Fermilab result of 2021 is [75, 76]

$$a_\mu^{\rm FL} = (116592040 \pm 54) \times 10^{-11}, \tag{4.19}$$

which, by itself, is a 3.3σ deviation from the SM prediction. Then, combining with the previous Brookhaven result one obtains [75, 76]

$$a_\mu^{\rm EXP} = (116592061 \pm 41) \times 10^{-11}, \tag{4.20}$$

which signals a 4.2σ deviation from the SM prediction,

$$\Delta a_\mu = a_\mu^{\rm EXP} - a_\mu^{\rm SM} = (251 \pm 59) \times 10^{-11}, \tag{4.21}$$

hinting towards a possible sign of NP. On the other hand, precise lattice QCD analysis [79] favors a result that is in accord with the SM prediction and is not included in the world average value that leads to the discrepancy of the SM with eq. (4.20). In this sense, it is still an open question whether the discrepancy of the anomalous magnetic moment is a sign of BSM physics or lack of proper understanding of the SM contributions.

Chapter 5

Flavour anomalies

In Chapter 2 we discussed the GIM mechanism, *i.e.* the suppression of FCNC-s, that originates from the hierarchy of the fermion masses and the unitarity of the CKM matrix in the SM. Due to this suppression, NP contributions invariably result in sizeable modifications to any processes involving FCNC-s.

In particular, the semileptonic decays of the B-meson provide the perfect arena for the search of NP effects where several deviations from the SM at the level of few sigmas remain relevant today (see *e.g.* [80, 81] for recent reviews). [1] One example of such processes is given by the decay of the B^+ meson into the K^+ meson and a ν-$\bar{\nu}$ pair.

At the quark level this process proceeds through the $b \to s\nu\bar{\nu}$ transition that is absent in the SM at tree level and is thus sensitive to any NP contributions beyond the SM. The Belle II collaboration has recently measured the branching ratio of the $B^+ \to K^+\nu\bar{\nu}$ process via two different techniques - the standard hadronic-tag (had) method and the newer inclusive-tag method (incl). The results are [82, 83]

$$\mathrm{BR}\left(B^+ \to K^+\bar{\nu}\nu\right)_{\mathrm{had}} = \left(1.1^{+0.9+0.8}_{-0.8-0.5} \times 10^{-5}\right), \tag{5.1}$$

$$\mathrm{BR}\left(B^+ \to K^+\bar{\nu}\nu\right)_{\mathrm{incl}} = (2.7 \pm 0.5 \pm 0.5) \times 10^{-5}, \tag{5.2}$$

where the errors represent the statistical and systematic uncertainties respectively. Combining these two results the Belle II measurements can be summarized as

$$\mathrm{BR}\left(B^+ \to K^+\bar{\nu}\nu\right)_{\mathrm{exp}} = (2.3 \pm 0.7) \times 10^{-6}. \tag{5.3}$$

Comparison of eq. (5.3) with the SM prediction in the absence of NP contributions [84, 85],

$$\mathrm{BR}(B^+ \to K^+\nu\bar{\nu})_{\mathrm{SM}} = (4.29 \pm 0.23) \times 10^{-6}, \tag{5.4}$$

[1] The quark content of the mesons considered in this Chapter has been summarized in Table 5.1.

signals a 2.7 σ deviation from the SM.

Meson	B^+	B^0	B_s^0	K^+	K^*	ϕ
Quark content	$u\bar{b}$	$d\bar{b}$	$s\bar{b}$	$u\bar{s}$	$d\bar{s}$	$s\bar{s}$

Table 5.1: Quark content of the mesons participating in flavour violating processes. The star superscript on K^* indicates that K^* is an off-shell K^0 meson.

Attributing this deviation to the effects of NP, we have

$$\mathrm{BR}(B^+ \to K^+ \bar{\nu}\nu)_{\mathrm{NP}} = (1.9 \pm 0.7) \times 10^{-5}. \tag{5.5}$$

There are two distinct ways in which the effects of NP may manifest in contributions to eq. (5.5).

The first option is to retain the assumption that the missing energy at Belle II experiment is carried away only by the SM neutrinos. In this case, the NP effects only appear indirectly due to heavy BSM particles that contribute to the Wilson coefficients of the effective operators, responsible for the flavour changing $b \to s\bar{\nu}\nu$ transition [86–95]. Due to the existing constraints from the $B^0 \to K^*\mu^+\mu^-$ and $B_s^0 \to \mu^+\mu^-$ decays, this scenario only works for models that introduce flavour non-universal couplings of the neutrinos to the NP fields [96, 97].

Alternatively, if the NP particles are light and long-lived enough they can escape the Belle II detector. Hence these NP particles can mimic the missing energy signature which is solely attributed to the SM neutrinos in the absence of NP [98–103].

In [103] the latter (direct) approach is examined by introducing a dark sector consisting of a dark photon and dark fermions. This model allows to explain the observed $B^+ \to K^+ E_{miss}$ excess while also satisfying the constraints for $B^0 \to K^* E_{miss}$ and predicting the branching ratio for $B_s^0 \to \phi\bar{\nu}\nu$, where E_{miss} denotes the missing energy observed at detectors. More details can be found in Chapter 6 and the article attached to this Thesis.

Chapter 6

Confronting the Standard Model with the dark photon

In Chapters 2 and 3 we discussed how different conceptual problems of the SM like the flavour hierarchy problem and the vacuum metastability of the Higgs potential hint towards the need for going beyond the canonical paradigm. Over the years, many different models addressing these issues have been proposed, making it very challenging to choose between the different realizations. Nevertheless, an easy way to identify more favourable models is to apply the principle of minimality by proposing that good models should explain as many conceptual or empirical issues of the SM as possible. Furthermore, they should also predict possible signatures at future experiments, thus making these models available for falsification.

A natural way of extending the SM is to propose the existence of a dark sector (DS) which is only weakly interacting with the SM thus avoiding stringent constraints from terrestrial collider experiments and cosmological observations. In this Thesis, we will briefly describe the model introduced in [67] in the context of the Higgs naturalness and the flavour hierarchy problem. We will show how this model can also change the stability properties of the Higgs potential and provide explanations for the recently observed flavour anomalies [44, 103].

6.1 Flavour hierarchy problem

The basic idea of this model, in the context of the flavour hierarchy problem, is to generate the exponential hierarchy of the fermion masses in the DS and then transmit this hierarchy to the SM via the messenger fields connecting the SM to the DS. The spontaneous breaking of the EW symmetry can be carried out in the DS by the Lee-Wick approach [104, 105] via the introduction of higher order derivatives for the gauge bosons of the

dark $U(1)_F$ symmetry, as shown in [106]. In particular, one introduces N_f dark fermions that are minimally coupled to the gauge bosons of the dark $U(1)_F$ symmetry. [1] The non-interacting part of the DS Lagrangian is then given by

$$\begin{aligned}\mathcal{L}_D = &-\frac{1}{4}F_{\mu\nu}F^{\mu\nu} + \frac{1}{\Lambda^2}\partial^\alpha F_{\alpha\mu}\partial^\beta F^\mu_\beta \\ &+ i\sum_{f=1}^{N_f}\bar{\psi}_f\gamma^\mu\left(\partial_\mu + ig\hat{Q}A_\mu\right)\psi_f,\end{aligned} \tag{6.1}$$

where $F_{\mu\nu} = \partial_\mu A_\nu - \partial_\nu A_\mu$ is the field strength tensor of the dark photon A_μ associated with the $U(1)_F$ symmetry, ψ_f are the N_f dark fermions, g is the coupling constant of $U(1)_F$ and $\hat{Q}$ is the charge operator defined by $\hat{Q}\psi_f = q_f\psi_f$. The mass spectrum of the dark fermions can then be determined by solving the mass gap equations, analogously to the Nambu-Jona-Lasinio mechanism, [106–108]

$$m_f = \Sigma(p, m_f)\big|_{p=m_f}, \tag{6.2}$$

where p is the momentum, m_f the mass of the fermion ψ_f and Σ the self energy introduced by the interaction of the dark fermions with the dark photon. At the leading order the solution of the mass gap equation is given by [106]

$$m_f = \Lambda\exp\left\{-\frac{8\pi^2}{3g^2(\Lambda)q_f^2} + \frac{1}{4}\right\}, \tag{6.3}$$

where the coupling constant g has been evaluated at the Lee-Wick scale Λ. It is immediately clear from eq. (6.3) that choosing order one flavour dependent charges q_f results in an exponential spread of the dark fermion masses. In order to solve the flavour hierarchy problem via this mechanism, three separate requirements must be satisfied. [2]

1. The DS must contain $2N_f$ fermions, where $N_f = 3$ denotes the number of quark generations in the SM. This is needed to reproduce a hierarchy in the DS analogous to the hierarchy in the SM quark masses. Following this similarity, we shall name the dark quarks $Q^{U,i}$ and Q^{D_i}, where $i = 1, 2, 3$.

[1] Here, by dark it is understood that no SM particles are charged under $U(1)_F$.

[2] The arguments given below can be used to explain the mass spectrum of both quarks and leptons. However, since previous work using this model has only focused on the mass generation of quarks, we choose to restrict ourselves to the quark hierarchy problem in this Thesis as well:

2. The SM flavour hierarchy problem originates from the unjustified introduction of dimensionless Yukawa couplings spanning several orders of magnitude. One way to avoid the hierarchy problem is to forbid these couplings at tree level and instead generate them at the loop level. To forbid the Yukawa couplings at tree level, a Z_2 symmetry can be introduced under which the Higgs transforms as $H \to -H$.

3. Once the flavour hierarchy has been generated in the DS, it should be transmitted to the SM. This can be done at 1-loop level via the messenger fields that connect the SM to the DS as mentioned before. The interaction Lagrangian of the messenger sector with the DS and the SM is given by

$$\begin{aligned}\mathcal{L}^I_{MS} = g_L &\left(\sum_{i=1}^{N_f} \bar{q}^i_L Q^{U_i}_R S^{U_i}_L + \sum_{i=1}^{N_f} \bar{q}^i_L Q^{D_i}_R S^{D_i}_L\right) \\ + g_R &\left(\sum_{i=1}^{N_f} \bar{u}^i_R Q^{U_i}_L S^{U_i}_R + \sum_{i=1}^{N_f} \bar{d}^i_R Q^{D_i}_L S^{D_i}_R\right) \\ + \lambda_S S_0 &\left(\tilde{H}^\dagger S^{U_i}_L S^{U_i}_R + H^\dagger S^{D_i}_L S^{D_i}_R\right) + h.c.,\end{aligned} \tag{6.4}$$

wherein q_L denotes the SM quark $SU(2)_L$ doublets, u_R, d_R the corresponding right-handed $SU(2)_L$ singlets, $Q^{U,D}_{L,R}$ denote the left (L) and right (R) handed components of the dark fermions introduced above, $S^{U,D}_L$ denote the scalar $SU(2)_L$ doublets and $S^{U,D}_R$ the corresponding $SU(2)_L$ singlet fields and g_L, g_R denote the corresponding Yukawa couplings. Finally, S_0 is a scalar that transforms as a singlet under both SM gauge group and the $U(1)_F$ symmetry and interacts with the SM Higgs doublet via the dimensionless coupling λ_S. The index i denotes the summation over the generations, whereas summation over the $SU(2)_L$ and $SU(3)_c$ indices has been left implicit.

Once the scalar singlet S_0 obtains a non-zero vacuum expectation value, $\langle S_0 \rangle = \mu$, the Yukawa couplings of the SM fermions to the Higgs doublet can be generated by 1-loop diagrams as explained in detail in [67]. The corresponding SM Yukawa couplings are given by

$$Y^q_i = \frac{g^q_L g^q_R}{16\pi^2} \left(\frac{M_{Q_i} \Lambda_S}{m^2}\right) f_1(x_i, \xi) \tag{6.5}$$

where the index i denotes the quark flavour and $f_1(x, \xi)$ is a loop function given by

$$f_1(x, \xi) = \frac{1}{2}\left[C_0\left(\frac{x}{1-\xi}\right)\frac{1}{1-\xi} + C_0\left(\frac{x}{1+\xi}\right)\frac{1}{1+\xi}\right], \tag{6.6}$$

with

$$C_0(x) = \frac{1 - x\,(1 - \log x)}{(1-x)^2}\,. \tag{6.7}$$

In the above equations, we defined $x_i = M_{Q_i}^2/m^2$, where m^2 is the average mass of the colored scalar messengers and M_{Q_i} is the mass of the dark fermion associated to the quark q^i. In addition, we introduced Λ_S and ξ indicating the scale of NP and the strength of the mixing in the colored messenger mass sector respectively:

$$\Lambda_S = \lambda_S v_S, \quad \xi = \frac{\Lambda_S v}{m^2}. \tag{6.8}$$

6.2 Vacuum stability

In Chapter 3 we showed how the Higgs potential is rendered metastable by the sizeable Yukawa coupling of the top quark to the Higgs doublet. This suggests that Higgs potential could be stable if the Higgs boson does not couple to the SM fermions at tree level. In the context of the DS model introduced in this Chapter, we have already seen that one way to solve the flavour hierarchy problem is to forbid the SM Yukawa couplings at tree level, in which case the experimentally observed Yukawa interactions are only effective operators generated at energies below the mass scale of the messenger fields. Therefore, above the scale $\tilde{m}$ the SM Yukawa couplings stop being local operators and thus do not affect the running of the Higgs quartic coupling λ_H, therefore having no effect on the stability of the Higgs potential.

In realistic solutions to the flavour hierarchy problem, the mass scale of the messenger fields is below the metastability scale of the Higgs potential $\tilde{m} < 10^{10}$ GeV, suggesting that the EW vev could correspond to the absolute minimum of the Higgs potential [44, 67]. In more detail, to assess the modifications of the DS and the messenger fields to the stability analysis, one needs to consider the running of λ_H as described in Chapter 3.

Before presenting the form of the β - function for λ_H, we delineate the potential for the scalar singlet S_0 introduced in the previous Section that obtains a non-zero vacuum expectation value $v_S >> v$, where v denotes the EW vev:[3]

$$V_{S_0} = \frac{\lambda_{S_0}}{4} S_0^4 - \frac{\mu_S^2}{2} S_0^2 + \frac{1}{2}\lambda_{HS} S_0^2 H^\dagger H. \tag{6.9}$$

As we shall see, the Higgs portal term λ_{HS} plays a particularly important role in enforcing the Higgs vacuum stability.

[3]The hierarchy in the vacuum expectation values is needed to suppress the experimentally constrained mixing angle between the Higgs boson and the scalar singlet.

In our analysis it was assumed that NP effects enter at the threshold scale $\tilde{m}$ above which the functional form of β_{λ_H} must be modified compared to the SM. In particular, at energies above $\tilde{m}$ the SM Yukawa couplings stop contributing to β_{λ_H} while new contributions associated with the heavy bosonic degrees of freedom must be included on top of the SM effects.

Thus at scales below $\tilde{m}$ we have at one loop

$$\begin{aligned}\beta^{(1)}_{\lambda_H} = 24\lambda_H^2 - 6y_t^4 + 12\lambda_H y_t^2 - \frac{9}{5}g'^2\lambda_H \\ -9g^2\lambda_H + \frac{27}{200}g'^4 + \frac{9}{20}g^2g'^2 + \frac{9}{8}g^4,\end{aligned} \tag{6.10}$$

where due to the flavour hierarchy of the Yukawa couplings, only the largest Yukawa coupling (y_t) is retained in the β function [44]. Above $\tilde{m}$ we have

$$\begin{aligned}\beta^{(1)}_{\lambda_H} = 24\lambda_H^2 + \frac{1}{2}\lambda_{HS}^2 - \frac{9}{5}g'^2\lambda_H \\ - 9g^2\lambda_H + \frac{27}{200}g'^4 + \frac{9}{20}g^2g'^2 + \frac{9}{8}g^4.\end{aligned} \tag{6.11}$$

As can be seen from eq. (6.11), above $\tilde{m}$, the value of the Higgs quartic coupling λ_H is increasing with energy due to the absence of the negative Yukawa contribution and the positive contribution from λ_{HS}. In [44] we carried out detailed numerical studies that confirmed this behavior quantitatively and showed that within the regime in which the model remains perturbatively unitary, the combination of these effects is sufficient to ensure Higgs vacuum stability either up to the Planck scale or up to the scale at which the first Landau pole appears.

6.3 Flavour anomalies

In Chapter 5 we described how the $B^+ \to K^+ E_{miss}$ transition may be explained by light NP if the associated particles are long-lived enough to escape detection thus exhibiting a missing energy signature. The DS model introduced in this Chapter provides the perfect arena for this type of set-up with the dark fermions providing the missing energy signature.

We assume the presence of N_f generations of dark fermions Q_i that are coupled to a massless dark photon A_D in close similarity to QED: [4]

$$\mathcal{L}_D \supset g_D \sum_i q_i \bar{Q}_i \gamma_\mu Q_i A_D^\mu. \tag{6.12}$$

[4] Here we are not focusing on reproducing the full hierarchy of the quark mass spectrum and thus the number of dark fermions may also be less than $2N_f$.

This interaction follows from the minimal coupling of the N_f dark fermions to the dark photon via the covariant derivative as described in Section 6.1. Furthermore, integrating out the heavy messenger fields also results in FCNC interaction between the dark photon and the b and s quarks

$$\mathcal{L}_{FCNC} \supset \frac{1}{2\Lambda}\bar{s}\sigma_{\mu\nu}bF_D^{\mu\nu}, \tag{6.13}$$

where $F_D^{\mu\nu} = \partial^\mu A_D^\nu - \partial^\nu A_D^\mu$ and $\sigma_{\mu\nu}$ was defined in Chapter 5. The effective scale Λ depends on the masses and couplings in the DS and the messenger sector, and its explicit form is given in [109]. Combining eqs. (6.12) and (6.13) we see that the $B^+ \to K^+ E_{miss}$ signature can be explained by the transition of B^+ to K^+ along with an off-shell photon, which yields a dark fermion-antifermion pair. As a side remark, we note that the simpler scenario of B^+ decaying to K^+ and an on-shell dark photon is not allowed by angular momentum conservation.

On the other hand, the production of a massless dark photon is allowed in the decay of B^0 meson into an excited state of the neutral Kaon, K^*, which has been measured by the Belle II and BaBar collaborations setting an experimental upper bound on the branching ratio $\mathrm{Br}(B^0 \to K^*\bar{\nu}\nu) < 2.7 \times 10^{-5}$ [110, 111] which in turn results in a lower bound on the scale $\Lambda \gtrsim 10^5$ GeV [103].

Setting $\Lambda \geq 10^5$ GeV, the observed branching ratio of $B^+ \to K^+ E_{miss}$ can be fitted with dark fermions with GeV-scale mass and $\alpha_D = (g_D^2)/(4\pi) \geq 0.5$. At a given scale Λ the minimum value of α_D required to fit the observed branching ratio decreases with an increasing number of dark fermion generations [103].

Fixing the cut-off scale at the lowest allowed value, $\Lambda \simeq 10^5$ GeV, also allows to infer an upper bound on the branching ratio of B_s^0 to ϕ and missing energy, where the BSM contribution to the missing energy signal is again provided by an on-shell dark photon (γ_D). In particular, in [103] we predicted that

$$Br(B_s^0 \to \phi\gamma_D) \lesssim 2 \times 10^{-5}, \tag{6.14}$$

in reach of future LHCb searches.

Chapter 7

New physics through higher spin particles

In the previous Chapter, we considered extending the SM by introducing a DS. In that case, we only included fields of the type that already exist within the SM, namely scalar and vector bosons and spin-1/2 fermions. However, an exhaustive search for NP should consider all the possible extensions, including fields with spin higher than 1. Therefore, in this Chapter we will exclusively focus on theories of higher spin fields, highlighting the theoretical problems and phenomenological applications. [1]

7.1 Brief overview of higher spin theories

As was mentioned before, the elementary particles of the SM have spin at most equal to 1. However, higher spin particles are also already known to exist in Nature as composite states of elementary particles with spin-1/2.

Indeed spin-3/2 particles have been observed as short-lived composite states bound by QCD. For example, the lightest of those particles, the Δ^{++} resonance, consists of three u-quarks and plays a key role in mediating interactions in low-energy QCD such as pion-nucleon scattering and pion photoproduction [112].

On top of spin-3/2 particles, the elementary spin-2 particles, known as gravitons are key ingredients of theories of quantum gravity. Nevertheless, a comprehensive description of the interactions between gravitons and the SM particles is still lacking.

In this Thesis, we will focus on the simplest case beyond the SM, considering only spin-3/2 particles. Rarita and Schwinger presented early attempts towards a field theoretic description of spin-3/2 in [113] building on

[1] From hereon, the term higher spin is meant to describe particles with spin $s > 1$.

the earlier work of Fierz and Pauli [114]. However, the Rarita-Schwinger theory was plagued by the inclusion of non-physical degrees of freedom, which had to be specifically projected to maintain the theory consistency. While a consistent projection operator could be identified for a free Rarita-Schwinger Lagrangian, it was soon shown that in gauged Rarita-Schwinger theories the complete removal of the unphysical degrees of freedom was impossible, potentially resulting in the violation of causality and perturbative unitarity [115, 116]. The first consistent description of interacting spin-3/2 fields was provided by supergravity [117–120]. In this case, the theory is equipped with supersymmetry that allows removing the unphysical degrees of freedom even in the presence of gauge interactions. The spin-3/2 field in supergravity, the gravitino is identified with the superpartner of the spin-2 graviton, possessing universal couplings to all lower spin fields [121, 122]. In addition, consistent non-supersymmetric proposals for spin-3/2 theories have also been studied. Early attempts in this direction were made in [123] specifically for non-derivative couplings. More recently [124] studied the propagation of spin-3/2 field in a constant electromagnetic background, avoiding the causality inconsistencies of Velo and Zwanziger [116]. Consistent theories of spin-3/2 fields have also been studied in the context of nuclear physics, wherein the unphysical degrees of freedom were absorbed by the contact terms in chiral perturbation theory [125–127]. However, in [128, 129] questions about the consistency of the theory outlined in [125–127] have been raised emphasizing the need for alternative formulations.

7.2 Multispinor formalism for higher spin fields

With the challenges of higher spin theories in mind, in this Section we propose a general formalism for dealing with higher spin fields that can be applied to fields with any integer or half-integer spin. This presents an opportunity for various applications as we will briefly summarize in the next Section.

The origin of the inconsistencies of higher spin theories is the excitation of non-physical degrees of freedom by the interaction terms. In field theory, the degrees of freedom of a field ψ are determined by its irreducible representations under the Lorentz group. Due to the isomorphism between the Lorentz algebra $so(3,1)$ and the algebra of the complex special linear group $sl(2,\mathbb{C})$, this amounts to a representation of a direct sum of two $su(2)$ algebras

$$so(1,3) \simeq su(2)_L \oplus su(2)_R, \tag{7.1}$$

which is characterized by a pair of integers (m,n) with the dimension of the

representation given by $(2m+1)(2n+1)$. On the other hand, a massive particle with spin j has $2(2j+1)$ physical degrees of freedom, as dictated by the Wigner little group [2] [130].

For spin-3/2, this amounts to $2(2\times 3/2+1)=8$ physical degrees of freedom, which should be contrasted by the $(1/2,1/2)\otimes((1/2,0)+(0,1/2))$ representation of Rarita and Schwinger that requires a $(2\times 1/2+1)(1/2\times 2+1)+2(1/2\times 2+1)=16$ dimensional representation. Hence, for Rarita-Schwinger theory, 8 unphysical degrees of freedom have to be projected out. [3] Alternatively, if one uses the $(3/2,0)\oplus(0,3/2)$ representation instead of the $(1/2,1/2)\otimes((1/2,0)\oplus(0,1/2))$ representation, the degrees of freedom $2(3/2\times 2+1)=8$ perfectly coincide with the physical case.

This insight was first used in practice in [131] to determine the consistent Feynman rules in perturbation theory for fields with arbitrary integer or half-integer spin. The main idea of such construction is to use the $(j,0)\oplus(0,j)$ representation for a field with spin j. Although for spin $j>1$ these representations do not admit a Lagrangian description, consistent Feynman rules in perturbation theory can still be derived if the following conditions are satisfied [131]:

1. Perturbation theory can be used to calculate the S-matrix from Dyson's formula [132]

$$S=\sum_{n=0}^{\infty}\frac{(-i)^n}{n!}\int_{-\infty}^{\infty}dt_1...dt_nT\{H'(t_1)...H'(t_n)\},\tag{7.2}$$

   where $T\{\}$ denotes the action of a time-ordering operator and the full Hamiltonian H has been split into the free Hamiltonian $H_0(t)$ and the interaction Hamiltonian $H'(t)$ and the interaction picture is used to define the time evolution of H':

$$H'(t)\equiv\exp(iH_0t)H(t=0)\exp(-iH_0t).\tag{7.3}$$

[2] The factor of 2 in front of 2j+1 comes from taking the antiparticles into account as well. For particles that are their own anti-particles such as Majorana fermions, this factor is not needed.

[3] In the discussion of this Thesis, we focus on the **real** representations, meaning representations for which $\psi_L=\psi_R^\dagger$ with L, and R alluding to the two Lie algebras in eq. (7.1) In this case, the physical degrees of freedom dictated by the Wigner group is 4 instead of 8, since each particle is its antiparticle and the number of degrees of freedom dictated by the Rarita-Schwinger representation is 8 instead of 16, since the representations of the $su(2)_L$ and $su(2)_R$ are not independent. For charged higher-spin particles one should instead consider **complex** representations, where the antiparticles double the degrees of freedom.

2. The S-matrix is Lorentz-invariant.

3. Particle interpretation may be used to construct the Hamiltonian density $\mathcal{H}(\mathbf{x}, t)$ from the creation and annihilation operators where $\mathcal{H}(\mathbf{x}, t)$ is defined by

$$H'(t) = \int \mathrm{d}^3 x \mathcal{H}(\mathbf{x}, t). \tag{7.4}$$

In the original formulation [131] the Feynman rules in the $(j, 0) \oplus (0, j)$ representation become ever more complicated with increasing j, raising the need for a more economical computational approach.

An alternative method using the original idea of [131] was thus put forth in [133] using the fact that every $(j, 0) \oplus (0, j)$ representation can be written as a symmetric tensor product of $(1/2, 0) \oplus (0, 1/2)$ representations. Thus a general spin-3/2 field in a $(j, 0) \oplus (0, j)$ representation can be written as

$$\psi_{(a)(\dot{a})} \equiv \psi_{(a_1 a_2 a_3)(\dot{a}_1 \dot{a}_2 \dot{a}_3)}, \tag{7.5}$$

where the brackets denote the symmetrization over the spinor indices, with the so-called multi-spinor indices a_i corresponding to the $(1/2, 0)$ representations and $\dot{a}_i$ corresponding to the $(0, 1/2)$ representations. The spinor indices (a) can be raised (lowered) with the appropriate Levi-Civita symbols $\epsilon^{(a)(b)}$ $(\epsilon_{(a)(b)})$. The raising and lowering for the dotted indices work analogously upon the replacement $(a) \to (\dot{a})$ and $(b) \to (\dot{b})$. Writing the fields in terms of the symmetrized tensor products of the fundamental representations of $su(2)_L \oplus su(2)_R$ simplifies the form of the Feynman rules considerably.

Even though the above method can be used to determine the Feynman rules for particles of any spin, in what follows we will provide the appropriate formulae only for the spin-3/2 field in the real representation. Using the symmetrized multispinor notation, the free spin-3/2 field $\psi_{(a)}$ can be written as a linear combination of plane waves as follows:

$$\psi_{(a)} = \int \frac{\mathrm{d}^3 p}{(2\pi)^3 (2E_{\mathrm{p}})} \sum_{\sigma} \left[a_{p\sigma} u_{(a)}(p, \sigma) e^{ipx} + a^*_{p\sigma} v_{(a)}(p, \sigma) e^{-ipx} \right], \tag{7.6}$$

wherein $E_p = \sqrt{\mathbf{p}^2 + m^2}$, $p = (E_{\mathbf{p}}, \mathbf{p})$, σ denotes the spin, and $u_{(a)}, v_{(a)}$ denote the symmetrized product of Weyl 2-spinors, where $(a) = (a_1 a_2 a_3)$. The creation operators a, a^* satisfy the canonical commutation relations:

$$\{a_{p\sigma}, a^*_{q\rho}\} = (2\pi)^3 (2E_{\mathbf{p}}) \delta_{\sigma\rho} \delta^3(\mathbf{p} - \mathbf{q}). \tag{7.7}$$

For explicit calculation of scattering amplitudes, one also needs to know the formulae for the spin sums. For the $(3/2, 0) \oplus (0, 3/2)$ representation these were first calculated in [131]. In the notation of [133] they become

$$\sum_{\sigma} u_{(a_1a_2a_3)}(p,\sigma)u^*_{(\dot{a}_1\dot{a}_2\dot{a}_3)}(p,\sigma) = \frac{p_{a_1\dot{a}_1}p_{a_2\dot{a}_2}p_{a_3\dot{a}_3}}{m^3}, \tag{7.8}$$

$$\sum_{\sigma} v_{(a_1a_2a_3)}(p,\sigma)v^*_{(\dot{a}_1\dot{a}_2\dot{a}_3)}(p,\sigma) = \frac{p_{a_1\dot{a}_1}p_{a_2\dot{a}_2}p_{a_3\dot{a}_3}}{m^3}, \tag{7.9}$$

$$\sum_{\sigma} u_{(a_1a_2a_3)}(p,\sigma)v^{(b_1b_2b_3)}(p,\sigma) = \delta^{(b_1b_2b_3)}_{(a_1a_2a_3)}, \tag{7.10}$$

where

$$p_{a\dot{a}} = \sigma^{\mu}_{a\dot{a}}p_{\mu}, \tag{7.11}$$

and

$$\sigma^{\mu}_{a\dot{a}} = (\mathbf{1}, \sigma^i), \tag{7.12}$$

where σ_i are the Pauli sigma matrices, for $i = 1, 2, 3$, $\mathbf{1}$ is the 2×2 identity matrix and $\delta^{(b)}_{(a)}$ denotes the symmetrized Kronecker delta. The Feynman rules for the external spin-3/2 lines and the spin-3/2 propagators are given in [133]. They are shown below:

Propagators

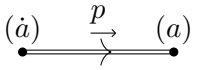

$= i\dfrac{p_{(a_1a_2a_3)(\dot{a}_1\dot{a}_2\dot{a}_3)}}{p^2 - m^2}$,
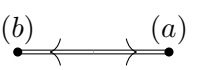

$= i\dfrac{m^3}{p^2 - m^2}\delta^{(b_1b_2b_3)}_{(a_1a_2a_3)}$,

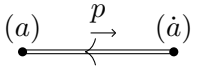

$= i\dfrac{p^{(\dot{a}_1\dot{a}_2\dot{a}_3)(a_1a_2a_3)}}{p^2 - m^2}$,
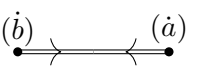

$= i\dfrac{m^3}{p^2 - m^2}\delta^{(\dot{a}_1\dot{a}_2\dot{a}_3)}_{(\dot{b}_1\dot{b}_2\dot{b}_3)}$.

External lines

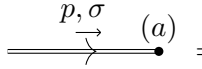

$= u_{(a_1a_2a_3)}(p,\sigma)$,
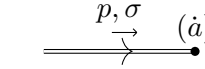

$= v^*_{(\dot{a}_1\dot{a}_2\dot{a}_3)}(p,\sigma)$,

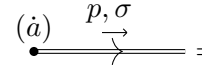

$= u^*_{(\dot{a}_1\dot{a}_2\dot{a}_3)}(p,\sigma)$,
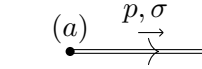

$= v_{(a_1a_2a_3)}(p,\sigma)$.

The free theory can then be perturbed by the inclusion of the Hamiltonian density for the interaction. In this way, since we assume that the Dyson series can be used, one can define the Feynman rules for the interaction vertices using the standard methods in perturbative quantum field theory [134]. Following the convention of [133] we assume that the spin-3/2 field has dimension 5/2, implying that every Lorentz invariant interaction

involving the spin-3/2 field must be non-renormalizable. Thus, all interactions between the spin-3/2 field and the SM fields are suppressed by the inverse powers of the cut-off scale Λ, corresponding to the scale of NP responsible for the origin of those couplings.

7.3 Phenomenology of spin-3/2 particles

Now we will describe some practical applications of the spin-3/2 theory in the minimal representation introduced in the previous Section.

In [133] the symmetrized multispinor formalism building on the original idea of Weinberg was used to investigate a spin-3/2 candidate for DM. In this case, the lowest-dimensional interaction that controls the evolution of the abundance of the spin-3/2 field is given by the Higgs portal term [133]:

$$\mathcal{H}_{\text{portal}} = -\frac{C_\lambda}{\Lambda^3}\psi^{(a_1a_2a_3)}\psi_{(a_1a_2a_3)}\left(|H|^2 - \frac{v^2}{2}\right), \tag{7.13}$$

where H denotes the Higgs doublet, v the Higgs vev, Λ the cut-off scale of the effective theory and C_λ is the Wilson coefficient of the portal operator. It was shown that while the spin-2 DM parameter space is tightly constrained by direct detection constraints for purely real Wilson coefficient C_λ, in the presence of complex Wilson coefficients, the direct detection constraints vanish instead, and the spin-3/2 particle can provide the totality of dark matter [133].

Spin-3/2 particles can also be searched for in collider experiments. In [135] the collider signatures for the interactions with the SM were identified. For a neutral, gauge singlet spin-3/2 field, the lowest order interactions are of dimension 7 and include the interactions with SM fermions, Higgs boson, or SM gauge bosons. It was shown that production channels for the spin-3/2 particles could be probed by the future lepton collider such as FCC and CLIC and by the high luminosity phase of the LHC [135].

One of the main topics for this Thesis is the search for NP through the anomalous magnetic moment of the muon. In [136] we considered the virtual contributions of spin-3/2 particles to a_μ introduced in Chapter 4. We found that the non-vanishing diagrams include a chirality flip on the external states, thus suppressing the contribution to a_μ. As a result, we inferred that spin-3/2 contributions are not enough to explain the deviation of a_μ from the SM values, meaning that the most promising channel to discover the higher spin particles is through high energy collider studies. In addition, by evaluating the electric dipole moments, we managed to put constraints on the spin-3/2 - electron couplings.

Finally, in [112] we used the $(3/2, 0) \oplus (0, 3/2)$ representation to study the interactions of the Δ^{++} - resonance with pions, nucleons and photons.

This work provided a useful example of a consistent higher spin theory for studying nuclear resonances. In the future, similar methods could be used also for other higher-spin hadronic resonances.

Chapter 8

Conclusion

The SM is presently the most successful theory of elementary particles and their interactions, having withstood an impressive amount of experimental tests over time. Nevertheless, it cannot be regarded as an ultimate description of physics at the fundamental level, since it leaves many conceptual and empirical questions unsolved. These issues call for studies of NP by including new fields and symmetries in addition to those already present within the SM. In view of minimality, preferred extensions of the SM should address as many shortcomings as possible. In this Thesis, we have studied 2 such models of NP, motivated by a variety of questions left unanswered by the SM.

In the first publication [135] we studied the contribution of spin-3/2 particles to the anomalous magnetic moment of the muon. We identified the appropriate dimension-7 couplings in the Hamiltonian and evaluated the 3 different loop diagrams that could contribute to the anomalous magnetic moment. We found that one of those diagrams is proportional to the square of the photon 4-momentum and thus vanishes on-shell while the other two diagrams are non-vanishing. The non-vanishing contributions to a_μ were found to be suppressed by the chirality flip on the external legs, limiting the effect on the value of a_μ. Hence, we concluded that the spin-3/2 particle by itself is not enough to explain the observed deviation of a_μ from its SM value. On the other hand, the contribution of the spin-3/2 particle on the electric dipole moments of leptons allowed placing mild constraints on the charge-parity violating part of the spin-3/2 couplings to the electron. From another perspective, the main novelty of this paper was to demonstrate practical loop computations using a consistent symmetric multispinor formalism for the first time. Aside from spin-3/2 contributions, we also evaluated the constraints from the measured value of a_μ for models with exotic fermions of spin-1/2.

We found that in contrast to the spin-3/2 case, spin-1/2 particles can easily explain the observed deviation of a_μ from its SM value.

The other two publications were dedicated to investigating the phenomenology of a DS model that can explain the observed hierarchy in quark masses and mixing as previously shown in [40, 43, 67, 109].

More specifically, in the second publication [44] we studied the aforementioned DS model in the context of Higgs vacuum stability. After computing the beta-functions at 1-loop, we then approximated the Higgs potential by its quartic interaction as described in Chapter 3 and studied the stability of the potential in two distinct scenarios. In the first scenario, the NP couplings at the mass scale of the messenger fields were initialized in such a way that no Landau poles were encountered until the Planck scale. It was found that the EW vacuum remained stable until the Planck scale. However, in this case, to correctly reproduce the empirically inferred value of the top quark Yukawa coupling, large values of the trilinear coupling between the Higgs boson and the messenger fields were needed, which resulted in the violation of perturbative unitarity in the scattering processes involving the messenger fields. To address this inconsistency we included a Lee-Wick (LW) higher derivative term [137, 138] that ensures perturbative unitarity provided that the messenger mass is sufficiently heavier than the mass of the LW ghost. We showed that the higher derivative extension does not alter our conclusions about Higgs vacuum stability. In the second scenario, we only considered values of the NP couplings for which perturbative values of the Higgs-messenger trilinear coupling are sufficient to match the top Yukawa coupling. Setting the trilinear coupling equal to the maximum value allowed by unitarity, we showed that vacuum stability can be ensured until the energy scale at which the first Landau pole is reached, which we identify with the UV cut-off of the theory. In both cases we explicitly verified that for our choice of parameters, the quartic couplings of the messenger fields remain positive throughout the RGE running, avoiding the emergence of color- and charge-breaking minima.

In the third publication [44] we explored the collider signatures of the DS model that can shed light on several conceptual issues of the SM such as the flavour hierarchy problem and the Higgs vacuum metastability problem. In particular, we focused on the flavour-violating decays of the B-mesons involving a massless dark photon. First by integrating out the messenger fields, we used the effective interaction between dark fermions and the dark photon to evaluate the branching ratio of the process $B^+ \to K^+ \bar{Q} Q$, including the Sommerfeld-Fermi corrections that resum the leading-log corrections to the relevant interaction vertices. Then we also evaluated the branching ratio for the process $B^0 \to K^* \gamma_D$. Since the on-shell dark photon can mimic the missing energy signature of the neutrino-antineutrino pair,

we then used the compatibility between experimentally measured branching ratio and the SM prediction for the process $B^0 \to K^* \bar{\nu}\nu$, to set a lower bound on the effective energy scale governing the interaction between the dark fermions and the dark photon. To address the tension between the SM and the experimentally inferred branching ratio for the $B^+ \to K^+ \nu\bar{\nu}$ process, we assumed that the missing energy signal observed in the experiment can result from the dark-fermion antifermion pair. We then showed that the process $B^+ \to K^+ \bar{Q}Q$ can perfectly reproduce the deviation observed in the decay $B^+ \to K^+ \bar{\nu}\nu$ for perturbative values for the dark gauge coupling and for dark fermions with sub-GeV masses. Finally, by predicting the branching ratio for the process $B_s^0 \to \phi\gamma_D$ we also provided a way to scrutinize our model in future collider experiments.

Overall, we investigated models of NP involving spin-0, spin-1/2, spin-1, and spin-3/2 particles. We found that simultaneously including new spin-0, spin-1/2 and spin-1 particles in the SM can provide explanations for conceptual problems of the SM, such as the flavour hierarchy problem and the Higgs vacuum metastability as well as empirical discrepancies between SM predictions and experiments. Concerning spin-3/2 fields, we presented a practical application of a consistent spin-3/2 theory by evaluating its contribution to the muon anomalous magnetic moment a_μ. Even though we saw that the spin-3/2 contribution is not sufficient to explain the deviation of the measured value of a_μ from the SM, our computation provided a practical example of consistent loop computations in a higher spin theory. Thus, our work may be a useful reference for further studies of open problems beyond the SM with spin-3/2 particles, such as explaining the matter-antimatter asymmetry through the decay of spin-3/2 particles.

Peatükk 9

Kokkuvõte: Standardmudeli edasiarenduste fenomenoloogilised järeldused

Standardmudel (SM) on kaasaegse fundamentaalfüüsika edukaim teooria elementaarosakeste omaduste ja vastastikmõjude kirjelduseks. Alates postuleerimisest on SM edukalt vastu pidanud kõikidele empiirilistele katsetele seda ümber lükata, ent vaatamata sellele ei saa SM-it siiski pidada osakestefüüsika lõplikuks kirjelduseks. Nimelt jätab SM lahendamata mitmed sisulised ning eksperimentaalsed küsimused, mis vihjavad uue füüsika olemasolule. Selle lõputöö kontekstis vaatleme SM edasiarendusi, kus olemasolevatele osakestele ja sümmeetriatele lisatakse uued osakesed ja sümmeetriad. Lähtudes minimaalsuse põhimõttest, tuleks uue füüsika mudelite valimisel eelistada neid, mis võimaldavad sama-aegselt lahendada rohkem kui ühe SM-i vajakajäämise. Enda lõputöö raames vaatlesin kahte võimalikku SM edasiarendust.

Esimeses artiklis [135] uurisime võimalikku muutust müooni anomaalses magnetmomendis spinn-3/2 osakeste tõttu. Esmalt määrasime kindlaks kõik vajalikud dimensioon-7 liikmed vastastikmõju Hamiltoniaanis ning siis arvutasime 3 silmusdiagrammi, mis võiksid potentsiaalselt müüoni anomaalsesse magnetmomenti a_μ panustada. Arvutuste tulemusena märkasime, et üks neist kolmest diagrammist on võrdeline footoni 4-impulssi ruuduga, mis massipinnal võrdub nulliga. Selgus, et ülejäänud kaks nullist erinevat panust on alla-surutud käelisuse-vahetuse poolt diagrammi välistel jalgadel, mistõttu on nende diagrammide panus a_μ-le väga väike. Seetõttu leidsime, et spinn-3/2 osakeste lisamine SM-le ei ole piisav, et seletada vaadeldud anomaalse magnetmomendi erinevust SM ennustustest. Lisaks

õnnestus meil arvutada spinn-3/2 osakeste panus elektroni dipoolmomendile, mis võimaldas mõõdukalt piirata elektroni laeng-paarsust rikkuvat vastastikmõju spinn-3/2 osakestega. Teisalt seisneb antud artikli kasutegur kooskõlalise spinn-3/2 teooria praktiliste rakenduste demonstreerimises. Nimelt esitasime artiklis [135] esimese näite silmusdiagrammide arvutamisest sümmeetrilise multispiinori teooria kontekstis. Võrdluseks vaatlesime ka eksootiliste spinn-1/2 osakeste panust a_μ-le. Erinevalt spinn-3/2 osakestest on uute spinn-1/2 osakestega võimalik lihtsasti vaadelud a_μ väärtust seletada.

Ülejäänud kahes artiklis uurisime tumeda sektori mudelit, mis võimaldab kirjeldada kvarkide masside ja segunemise hierarhiat [40, 44, 67, 109].

Täpsemalt uurisime teises artiklis [44] ülalmainitud tumeda sektori mudelit Higgsi vaakumi stabiilsuse kontekstis. Olles arvutanud antud teooria beta-funktsioonid 1 silmuse tasemel, lähendasime Higgsi potentsiaali neljapunkti interaktsiooniga nagu kirjeldasime peatükis 3 ning seejärel kasutasime saadud lähendust, et uurida Higgsi potentsiaali stabiilsust, käsitledes kahte võimalikku stsenaariumit. Esmalt lähtestasime uute osakeste mõjukonstandid viisil, mis võimaldaks vältida Landau pooluseid kuni Plancki skaalani. Leidsime, et elektronõrk vaakum püsib stabiilsena kuni Plancki skaalani. Samal ajal aga märkasime, et sellistel tingimustel on võimalik top kvargi Yukawa konstanti ühildada vaatlustulemustega ainult juhul, kui kolmepunkti vastastikmõju määrav konstant Higgsi ja skalaarvahendajaväljade vahel omandab väga kõrged väärtused. Need väärtused on problemaatilised teooria kooskõlalisusele, kuna kätkevad endas unitaarsuse rikkumist vahendajaskalaaride hajumisel. Selle probleemi lahendamiseks lisasime teooriale Lee-Wick kõrgemat järku tuletisega liikme [137, 138], mis tagas unitaarsuse juhul, kui vahendajaskalaaride mass on raskem kui Lee-Wick tontvälja mass. Näitasime otsese arvutuse teel, et kõrgemat järku tuletisega liige ei mõjuta meie varasemaid tulemusi vaakumi stabiilsuse kohta. Teisel juhul vaatlesime olukorda, kus kolmepunkti seosekonstant omandas häiritusteoreetilise unitaarsusega kooskõlalised väärtused. Olles kolmepunkti seoskonstandi fikseerinud maksimaalsele väärtusele, mis rahuldaks siiski häiritusteoreetilise unitaarsuse tingimusi, näitasime, et antud juhul on Higgsi stabiilsus samuti tagatud esimese Landau pooluse ilmnemiseni. Mõlemal juhul tegime kindlaks, et vahendajaskalaaride neljapunkti seoskonstandid jääksid positiivseks kogu vaadeldud renormeerimisrühme võrrandite jooksmise puhul, vältimaks värvi- ja laengusümmeetriat rikkuvaid skalaarpotentsiaali miinimume.

Kolmandas artiklis [103] uurisime eelnevalt vaadeldud tumeda sektori omadusi kiirendifüüsika eksperimentide kontekstis. Põhiliselt keskendusime lõhna-sümmeetriat rikkuvate B-mesoni lagunemiskanalitele. Esmalt vaatlesime efektiivset vastastikmõju tumedate fermionite ja massitu tumeda footoni vahel, mis tekib raskete skalaarvahendajate väljaintegreerimise tu-

lemusena. Rakendasime antud vastastikmõju, et arvutada $B^+ \to K^+\bar{Q}Q$ hargnemissuhe, võttes arvesse Sommerfeld-Fermi parandeid, et taasliita esimest järku logaritmilised parandid. Seejärel arvutasime hargnemissuhte ka $B^0 \to K^*\gamma_D$ protssesi jaoks. Kuna massipinnal olev tumefooton jäljendab kiirendis vaadeldud puuduoleva energia jälge sarnaselt neutriino-antineutriino paariga protsessis $B^0 \to K^*\bar{\nu}\nu$, saime kasutatada SM ja eksperimentaalsete vaatluste kooskõlalisust, seadmaks alampiiri uue füüsika energiaskaalale, mis omakorda mõjutab tumedate fermionide ja tumeda footoni interaktsiooni tugevust. Järgmisena pöörasime tähelepanu $B^+ \to K^+\bar{\nu}\nu$ hargnemissuhtele. Seletamaks antud protsessi eksperimentaalselt tuletatud hargnemissuhte erinevust SM-i ennustusest, eeldasime, et sel juhul jäljendab kadunud energia signaali kerge massiga fermion-antifermion paar. Sellest lähtuvalt näitasime, et protsess $B^+ \to K^+\bar{Q}Q$ sobib ideaalselt seletamaks eksperimentaalselt vaadeldud $B^+ \to K^+\nu\bar{\nu}$ hargnemissuhet, kuivõrd osa neutriino-antineutriino paarile omastatud kadunud energiast tuleks tegelikult samastada fermion-antifermion paari panusega. Näitasime, et antud seletust saab muuhulgas rakendada juhul kui seoskonstantidel on häiritusteooriaga kooskõlalised väärtused, ning et tumedate fermionite mass on pisut väiksem kui GeV. Viimaks esitasime mudelist johtuva ennustuse $B_s^0 \to \phi\gamma_D$ hargnemissuhte jaoks, mis võimaldab meie mudelit tulevikueksperimentide abil kontrollida.

Kokkuvõttes uurisime uue füüsika mudeleid, mis hõlmasid spinn-0, spinn-1/2, spinn-1 ja spinn-3/2 osakesi. Leidsime, et SM-le samaaegselt uute spinn-0, spinn-1/2 ja spinn-1 osakeste lisamine võimaldab seletada SM-i sisulisi vajakajäämisi nagu lõhnahierarhia probleem ja Higgsi vaakumi metastabiilsus ning ühtlasi empiirilisi erinevusi SM-i ja eksperimentaalsete tulemuste vahel. Spinn-3/2 osakeste kontekstis esitasime praktilise näite kooskõlalise spinn-3/2 teooria kasutamisest, arvutades antud osakese panuse müüoni anomaalsele magnetmomendile a_μ. Kuigi ilmnes, et spinn-3/2 panus iseseisvalt ei ole piisav, et seletada eksperimentaalselt mõõdetud a_μ erinevust SM-ist, pakkus meie arvutus sellegipoolest välja kasuliku näite silmusdiagrammide arvutamisest kooskõlalise kõrgema spinni teooria kontekstis. Seetõttu võib meie töö spinn-3/2 osakeste alal osutuda kasulikuks viiteks kõrgema spinni teooria rakendamisel teiste SM-i probleemide adresseerimiseks. Üks lihtne näide potentsiaalsetest kõrgema spinni teooria rakendusest tulevikku silmas pidadades on aine-antiaine asümmeetria, mis võib olla seletatav läbi spinn-3/2 osakeste lagunemise.

Bibliography

[1] Serguei Chatrchyan et al. Observation of a New Boson at a Mass of 125 GeV with the CMS Experiment at the LHC. *Phys. Lett. B*, 716:30–61, 2012.

[2] Georges Aad et al. Observation of a new particle in the search for the Standard Model Higgs boson with the ATLAS detector at the LHC. *Phys. Lett. B*, 716:1–29, 2012.

[3] Y. Fukuda et al. Evidence for oscillation of atmospheric neutrinos. *Phys. Rev. Lett.*, 81:1562–1567, 1998.

[4] C. A. Baker, D. D. Doyle, P. Geltenbort, K. Green, M. G. D. van der Grinten, P. G. Harris, P. Iaydjiev, S. N. Ivanov, D. J. R. May, J. M. Pendlebury, J. D. Richardson, D. Shiers, and K. F. Smith. Improved experimental limit on the electric dipole moment of the neutron. *Phys. Rev. Lett.*, 97:131801, Sep 2006.

[5] J. Wess and B. Zumino. Supergauge Transformations in Four-Dimensions. *Nucl. Phys. B*, 70:39–50, 1974.

[6] Pierre Fayet. Spontaneously Broken Supersymmetric Theories of Weak, Electromagnetic and Strong Interactions. *Phys. Lett. B*, 69:489, 1977.

[7] R. D. Peccei and Helen R. Quinn. CP Conservation in the Presence of Instantons. *Phys. Rev. Lett.*, 38:1440–1443, 1977.

[8] F. Wilczek. Problem of strong p and t invariance in the presence of instantons. *Phys. Rev. Lett.*, 40:279–282, Jan 1978.

[9] Steven Weinberg. A new light boson? *Phys. Rev. Lett.*, 40:223–226, Jan 1978.

[10] Gerard Jungman, Marc Kamionkowski, and Kim Griest. Supersymmetric dark matter. *Phys. Rept.*, 267:195–373, 1996.

[11] L. F. Abbott and P. Sikivie. A Cosmological Bound on the Invisible Axion. *Phys. Lett. B*, 120:133–136, 1983.

[12] Michael Dine and Willy Fischler. The Not So Harmless Axion. *Phys. Lett. B*, 120:137–141, 1983.

[13] J.Iliopoulos S.L.Glashow and L.Maiani. Weak Interactions with Lepton-Hadron Symmetry. *Phys. Rev. D*, 2:1285, 1970.

[14] B.Abi et al. Measurement of the positive muon anomalous magnetic moment to 0.46ăppm. *Physical Review Letters*, 126(14), April 2021.

[15] F. Englert and R. Brout. Broken symmetry and the mass of gauge vector mesons. *Phys. Rev. Lett.*, 13:321–323, Aug 1964.

[16] Peter W. Higgs. Broken symmetries and the masses of gauge bosons. *Phys. Rev. Lett.*, 13:508–509, Oct 1964.

[17] G. S. Guralnik, C. R. Hagen, and T. W. B. Kibble. Global conservation laws and massless particles. *Phys. Rev. Lett.*, 13:585–587, Nov 1964.

[18] Giuseppe Degrassi, Stefano Di Vita, Joan Elias-Miro, Jose R. Espinosa, Gian F. Giudice, Gino Isidori, and Alessandro Strumia. Higgs mass and vacuum stability in the Standard Model at NNLO. *JHEP*, 08:098, 2012.

[19] Steven Weinberg. A model of leptons. *Phys. Rev. Lett.*, 19:1264–1266, Nov 1967.

[20] S. L. Glashow. Partial Symmetries of Weak Interactions. *Nucl. Phys.*, 22:579–588, 1961.

[21] Abdus Salam. Weak and Electromagnetic Interactions. *Conf. Proc. C*, 680519:367–377, 1968.

[22] P. Langacker. *The Standard Model and Beyond*. CRC Press, A Taylor and Francis Group, 2010.

[23] C.N.Yang and R.L.Mills. Conservation of Isotopic Spin and Isotopic Gauge Invariance. *Phys. Rev.*, 96:191, 1954.

[24] D.J.Gross and F.Wilczek. Ultraviolet Behavior of Non-Abelian Gauge Theories. *Phys. Rev. Lett.*, 30:1343, 1973.

[25] D.J.Gross and F.Wilczek. Asymptotically Free Gauge Theories. I. *Phys. Rev. D*, 8:3633, 1973.

[26] D.J.Gross and F.Wilczek. Asymptotically Free Gauge Theories. II. *Phys. Rev. D*, 9:980, 1974.

[27] Jeffrey Goldstone, Abdus Salam, and Steven Weinberg. Broken symmetries. *Phys. Rev.*, 127:965–970, Aug 1962.

[28] M.K.Gaillard J. Ellis and D.V.Nanopoulus. A Historical Profile of the Higgs Boson. arXiv:1201.6045v1 [hep-ph], 2012.

[29] C. Giunti and C.W.Kim. *Fundamentals of Neutrino Physics and Astrophysics*. Oxford University Press, 2007.

[30] H. E. Logan. TASI 2013 Lectures on Higgs Physics Within and Beyond the SM. arXiv:1406.1786v2 [hep-ph], 2014.

[31] T. Nakano and K. Nishijima. Charge Independence for V-Particles. *Prog. of Theor. Phys.*, 10:581, 1953.

[32] B. Pontecorvo. Inverse beta processes and nonconservation of lepton charge. *Zh. Eksp. Teor. Fiz.*, 34:247, 1957.

[33] Ziro Maki, Masami Nakagawa, and Shoichi Sakata. Remarks on the Unified Model of Elementary Particles. *Progress of Theoretical Physics*, 28(5):870–880, 11 1962.

[34] Pablo Martínez-Miravé, Kristjan Müürsepp, and Mariam Tortola. Neutrino physics. *PoS*, CORFU2021:321, 2022.

[35] N. Cabibbo. Unitary Symmetry and Leptonic Decays. *Phys. Rev. Lett.*, 10:531, 1963.

[36] M.Kobayashi and T.Maskawa. CP Violation in the Renormalizable Theory of the Weak Interaction. *Prog. of Theor. Phys.*, 49:652, 1973.

[37] L-L Chau and W-Y Keung. Comments on the Parametrization of the Kobayashi-Maskawa Matrix. *Phys. Rev. Lett.*, 53:1802, 1984.

[38] M.Tanabashi *et al.* (Particle Data Group). *Phys. Rev. D*, 98:03001, 2018 and 2019 Update.

[39] R. L. Workman and Others. Review of Particle Physics. *PTEP*, 2022:083C01, 2022.

[40] Kristjan Müürsepp. The flavor hierarchy problem in the standard model and beyond the standard model theories. Master's thesis, University of Tartu, 2020.

[41] Ferruccio Feruglio. Pieces of the Flavour Puzzle. *The European Physical Journal C*, 75(8), 2015.

[42] Emidio Gabrielli, Luca Marzola, and Martti Raidal. Radiative Yukawa Couplings in the Simplest Left-Right Symmetric Model. *Phys. Rev. D*, arXiv: 1611.00009 [hep-ph](3):035005, 2017.

[43] Emidio Gabrielli, Carlo Marzo, Luca Marzola, and Kristjan Müürsepp. Dark origin of the quark flavor hierarchy and mixing. *Phys. Rev. D*, 101(7):075019, 2020.

[44] Emidio Gabrielli, Luca Marzola, Kristjan Müürsepp, and Ruiwen Ouyang. Vacuum stability with radiative Yukawa couplings. *JHEP*, 01:142, 2022.

[45] C. D. Froggatt and Holger Bech Nielsen. Hierarchy of Quark Masses, Cabibbo Angles and CP Violation. *Nucl. Phys. B*, 147:277–298, 1979.

[46] Pierre Binetruy, Stephane Lavignac, and Pierre Ramond. Yukawa textures with an anomalous horizontal Abelian symmetry. *Nucl. Phys. B*, 477:353–377, 1996.

[47] S. F. King and Graham G. Ross. Fermion masses and mixing angles from SU(3) family symmetry. *Phys. Lett. B*, 520:243–253, 2001.

[48] Yohei Ema, Koichi Hamaguchi, Takeo Moroi, and Kazunori Nakayama. Flaxion: a minimal extension to solve puzzles in the standard model. *JHEP*, 01:096, 2017.

[49] Federica Bazzocchi, Luca Merlo, and Stefano Morisi. Fermion Masses and Mixings in a S(4)-based Model. *Nucl. Phys. B*, 816:204–226, 2009.

[50] Cheng-Wei Chiang and Kei Yagyu. Radiative Seesaw Mechanism for Charged Leptons. *Phys. Rev. D*, 103(11):L111302, 2021.

[51] S. Alekhin, A. Djouadi, and S. Moch. The top quark and Higgs boson masses and the stability of the electroweak vacuum. *Phys. Lett. B*, 716:214–219, 2012.

[52] Dario Buttazzo, Giuseppe Degrassi, Pier Paolo Giardino, Gian F. Giudice, Filippo Sala, Alberto Salvio, and Alessandro Strumia. Investigating the near-criticality of the Higgs boson. *JHEP*, 12:089, 2013.

[53] J. Ellis, J. R. Espinosa, G. F. Giudice, A. Hoecker, and A. Riotto. The Probable Fate of the Standard Model. *Phys. Lett. B*, 679:369–375, 2009.

[54] Joan Elias-Miro, Jose R. Espinosa, Gian F. Giudice, Hyun Min Lee, and Alessandro Strumia. Stabilization of the Electroweak Vacuum by a Scalar Threshold Effect. *JHEP*, 06:031, 2012.

[55] Vincenzo Branchina and Emanuele Messina. Stability, Higgs Boson Mass and New Physics. *Phys. Rev. Lett.*, 111:241801, 2013.

[56] Aneesh V. Manohar and Emily Nardoni. Renormalization Group Improvement of the Effective Potential: an EFT Approach. *JHEP*, 04:093, 2021.

[57] Ya. B. Zeldovich, I. Yu. Kobzarev, and L. B. Okun. Cosmological Consequences of the Spontaneous Breakdown of Discrete Symmetry. *Zh. Eksp. Teor. Fiz.*, 67:3–11, 1974.

[58] R. Jackiw. Functional evaluation of the effective potential. *Phys. Rev. D*, 9:1686, 1974.

[59] Mariano Quiros. Finite temperature field theory and phase transitions. In *ICTP Summer School in High-Energy Physics and Cosmology*, volume arXiv: 9901312 [hep-ph], pages 187–259, 1 1999.

[60] Sidney R. Coleman and Erick J. Weinberg. Radiative Corrections as the Origin of Spontaneous Symmetry Breaking. *Phys. Rev. D*, 7:1888–1910, 1973.

[61] Curtis G. Callan. Broken scale invariance in scalar field theory. *Phys. Rev. D*, 2:1541–1547, Oct 1970.

[62] K. Symanzik. Small distance behavior in field theory and power counting. *Commun. Math. Phys.*, 18:227–246, 1970.

[63] K. Symanzik. Small distance behavior analysis and Wilson expansion. *Commun. Math. Phys.*, 23:49–86, 1971.

[64] Marc Sher. Electroweak Higgs Potentials and Vacuum Stability. *Phys. Rept.*, 179:273–418, 1989.

[65] Manfred Lindner, Marc Sher, and Helmut W. Zaglauer. Probing Vacuum Stability Bounds at the Fermilab Collider. *Phys. Lett. B*, 228:139–143, 1989.

[66] Ming-xing Luo and Yong Xiao. Two loop renormalization group equations in the standard model. *Phys. Rev. Lett.*, 90:011601, 2003.

[67] Emidio Gabrielli and Martti Raidal. Exponentially spread dynamical Yukawa couplings from nonperturbative chiral symmetry breaking in the dark sector. *Phys. Rev. D*, 89(1):015008, 2014.

[68] Aharon Davidson and Kameshwar C. Wali. Universal seesaw mechanism? *Phys. Rev. Lett.*, 59:393–395, Jul 1987.

[69] Subhash Rajpoot. Chirally Symmetric Strong and Electroweak Interactions. *Phys. Lett. B*, 208:483–486, 1988.

[70] Z.G. Berezhiani and R. Rattazzi. Universal seesaw and radiative quark mass hierarchy. *Physics Letters B*, 279(1):124–130, 1992.

[71] P. S. Bhupal Dev, Rabindra N. Mohapatra, and Yongchao Zhang. Quark Seesaw, Vectorlike Fermions and Diphoton Excess. *JHEP*, 02:186, 2016.

[72] Paul A. M. Dirac. The quantum theory of the electron. *Proc. Roy. Soc. Lond. A*, 117:610–624, 1928.

[73] Julian S. Schwinger. On Quantum electrodynamics and the magnetic moment of the electron. *Phys. Rev.*, 73:416–417, 1948.

[74] Fred Jegerlehner and Andreas Nyffeler. The Muon g-2. *Phys. Rept.*, 477:1–110, 2009.

[75] Chris Polly. Muon g-2 results. Talk given at Fermilab, April 7, 2021.

[76] B. Abi et al. Measurement of the Positive Muon Anomalous Magnetic Moment to 0.46 ppm. *Phys. Rev. Lett.*, 126:141801, 4 2021.

[77] G. W. Bennett et al. Final Report of the Muon E821 Anomalous Magnetic Moment Measurement at BNL. *Phys. Rev. D*, 73:072003, 2006.

[78] T. Aoyama et al. The anomalous magnetic moment of the muon in the Standard Model. *Phys. Rept.*, 887:1–166, 2020.

[79] Sz. Borsanyi et al. Leading hadronic contribution to the muon magnetic moment from lattice QCD, Nature (April 7, 2021).

[80] Monika Blanke. *B* Physics: From Present to Future Colliders. In *23rd Hellenic School and Workshops on Elementary Particle Physics and Gravity*, volume arxiv/, 3 2024.

[81] David London and Joaquim Matias. B-Flavor anomalies: 2021 theoretical status report. *Annual Review of Nuclear and Particle Science*, 72(1):3768, September 2022.

[82] Belle-II. Evidence for $B^+ \to K^+\nu\bar{\nu}$ Decays. arXiV: 2311.14647 [hep-ex], Belle II Preprint 2023-017, KEK Preprint 2023-35, 11 2023.

[83] E. Ganiev. https : //indico.desy.de/event/34916/contributions/146877/. Paralell talk given at the EPS-HEP2023 Conference in Hamburg (Germany, Aug 20-25, 2023).

[84] Wolfgang Altmannshofer, Andrzej J. Buras, David M. Straub, and Michael Wick. New strategies for New Physics search in $B \to K^*\nu\bar{\nu}$, $B \to K\nu\bar{\nu}$ and $B \to X_s\nu\bar{\nu}$ decays. *JHEP*, 04:022, 2009.

[85] Andrzej J. Buras, Jennifer Girrbach-Noe, Christoph Niehoff, and David M. Straub. $B \to K^{(*)}\nu\overline{\nu}$ decays in the Standard Model and beyond. *JHEP*, 02:184, 2015.

[86] Rigo Bause, Hector Gisbert, and Gudrun Hiller. Implications of an enhanced $B \to K\nu\bar{\nu}$ branching ratio. arXiv:2309.00075 [hep-ph], 2023.

[87] Peter Athron, R. Martinez, and Cristian Sierra. B meson anomalies and large $B^+ \to K^+\overline{\nu}\nu$ in non-universal u(1) models. *Journal of High Energy Physics*, 2024(2), February 2024.

[88] Xiao-Gang He, Xiao-Dong Ma, and German Valencia. Revisiting models that enhance $B^+ \to K^+\nu\bar{\nu}$ in light of the new Belle II measurement. arXiv: 2309.12741 [hep-ph], 9 2023.

[89] Alakabha Datta, Danny Marfatia, and Lopamudra Mukherjee. B→K$\nu\nu^-$, MiniBooNE and muon g-2 anomalies from a dark sector. *Phys. Rev. D*, 109(3):L031701, 2024.

[90] Feng-Zhi Chen, Qiaoyi Wen, and Fanrong Xu. Correlating $B \to K^{(*)}\nu\bar{\nu}$ and flavor anomalies in SMEFT. arXiv: 2401.11552 [hep-ph], 2024.

[91] Lukas Allwicher, Damir Becirevic, Gioacchino Piazza, Salvador Rosauro-Alcaraz, and Olcyr Sumensari. Understanding the first measurement of B(B→K$\nu\nu^-$). *Phys. Lett. B*, 848:138411, 2024.

[92] Chuan-Hung Chen and Cheng-Wei Chiang. Flavor anomalies in leptoquark model with gauged $U(1)_{L_\mu - L_\tau}$. arXiv: 2309.12904 [hep-ph], 9 2023.

[93] Biao-Feng Hou, Xin-Qiang Li, Meng Shen, Ya-Dong Yang, and Xing-Bo Yuan. Deciphering the Belle II data on $B \to K\nu\bar{\nu}$ decay in the (dark) SMEFT with minimal flavour violation. arXiv:2402.19208 [hep-ph], 2 2024.

[94] Xiao-Gang He, Xiao-Dong Ma, Michael A. Schmidt, German Valencia, and Raymond R. Volkas. Scalar dark matter explanation of the excess in the Belle II $B^+ \to K^+ +$ invisible measurement. arXiv:2403.12485 [hep-ph], 3 2024.

[95] Tobias Felkl, Anjan Giri, Rukmani Mohanta, and Michael A. Schmidt. When energy goes missing: new physics in $b \to s\nu\nu$ with sterile neutrinos. *Eur. Phys. J. C*, 83(12):1135, 2023.

[96] Marcel Algueró, Aritra Biswas, Bernat Capdevila, Sébastien Descotes-Genon, Joaquim Matias, and Martin Novoa-Brunet. To (b)e or not to (b)e: no electrons at LHCb. *The European Physical Journal C*, 83(7), July 2023.

[97] Sébastien Descotes-Genon, Svjetlana Fajfer, Jernej F. Kamenik, and Martín Novoa-Brunet. Implications of $b \to s\mu\mu$ anomalies for future measurements of $B \to K^{(*)}\nu\bar{\nu}$ and $K \to \pi\nu\bar{\nu}$. *Phys. Lett. B*, 809:135769, 2020. [Addendum: Phys.Lett.B 840, 137830 (2023)].

[98] Sebastian Bruggisser, Lara Grabitz, and Susanne Westhoff. Global analysis of the ALP effective theory. *JHEP*, 01:092, 2024.

[99] Alexander Berezhnoy and Dmitri Melikhov. $B \to K^* M_X$ vs $B \to K M_X$ as a probe of a scalar-mediator dark matter scenario. *EPL*, 145(1):14001, 2024.

[100] Wolfgang Altmannshofer, Andreas Crivellin, Huw Haigh, Gianluca Inguglia, and Jorge Martin Camalich. Light New Physics in $B \to K^{(*)}\nu\bar{\nu}$? arXiv : 2311.14629[hep-ph], PSI-PR-23-46, ZU-TH 77/23, 11 2023.

[101] Kåre Fridell, Mitrajyoti Ghosh, Takemichi Okui, and Kohsaku Tobioka. Decoding the $B \to K\nu\nu$ excess at Belle II: kinematics, operators, and masses. arXiv:2312.12507 [hep-ph], 2023.

[102] David McKeen, John N. Ng, and Douglas Tuckler. Higgs Portal Interpretation of the Belle II $B^+ \to K^+\nu\nu$ Measurement. arXiv:2312.00982 [hep-ph], 2023.

[103] Emidio Gabrielli, Luca Marzola, Kristjan Müürsepp, and Martti Raidal. Explaining the $B^+ \to K^+\nu\bar{\nu}$ excess via a massless dark photon. *Eur. Phys. J. C*, 84(5):460, 2024.

[104] T. D. Lee and G. C. Wick. Finite theory of quantum electrodynamics. *Phys. Rev. D*, 2:1033–1048, Sep 1970.

[105] Benjamín Grinstein, Donal OConnell, and Mark B. Wise. The Lee-Wick standard model. *Physical Review D*, 77(2), January 2008.

[106] Emidio Gabrielli. On the dynamical breaking of chiral symmetry: A New mechanism. *Phys. Rev. D*, 77:055020, 2008.

[107] Y. Nambu and G. Jona-Lasinio. Dynamical model of elementary particles based on an analogy with superconductivity. I. *Phys. Rev.*, 122:345–358, Apr 1961.

[108] Y. Nambu and G. Jona-Lasinio. Dynamical model of elementary particles based on an analogy with superconductivity. II. *Phys. Rev.*, 124:246–254, Oct 1961.

[109] Emidio Gabrielli, Barbara Mele, Martti Raidal, and Elena Venturini. FCNC decays of standard model fermions into a dark photon. *Physical Review D*, 94(11), December 2016.

[110] J. Grygier et al. Search for $\boldsymbol{B \to h\nu\bar{\nu}}$ decays with semileptonic tagging at Belle. *Phys. Rev. D*, 96(9):091101, 2017. [Addendum: Phys.Rev.D 97, 099902 (2018)].

[111] J. P. Lees et al. Search for $B \to K^{(*)}\nu\overline{\nu}$ and invisible quarkonium decays. *Phys. Rev. D*, 87(11):112005, 2013.

[112] Juan Carlos Criado, Abdelhak Djouadi, Niko Koivunen, Kristjan Müürsepp, Martti Raidal, and Hardi Veermäe. An effective field theory of the Delta-resonance. arXiV:2106.09031 [hep-ph], 6 2021.

[113] William Rarita and Julian Schwinger. On a theory of particles with half integral spin. *Phys. Rev.*, 60:61, 1941.

[114] M. Fierz and W. Pauli. On relativistic wave equations for particles of arbitrary spin in an electromagnetic field. *Proc. Roy. Soc. Lond. A*, 173:211–232, 1939.

[115] Kenneth Johnson and E. C. G. Sudarshan. Inconsistency of the local field theory of charged spin 3/2 particles. *Annals Phys.*, 13:126–145, 1961.

[116] Giorgio Velo and Daniel Zwanzinger. Noncausality and other defects of interaction lagrangians for particles with spin one and higher. *Phys. Rev.*, 188:2218–2222, Dec 1969.

[117] Daniel Z. Freedman, P. van Nieuwenhuizen, and S. Ferrara. Progress Toward a Theory of Supergravity. *Phys. Rev. D*, 13:3214–3218, 1976.

[118] Stanley Deser and B. Zumino. Consistent Supergravity. *Phys. Lett. B*, 62:335, 1976.

[119] Daniel Z. Freedman and P. van Nieuwenhuizen. Properties of supergravity theory. *Phys. Rev. D*, 14:912–916, Aug 1976.

[120] P. Van Nieuwenhuizen. Supergravity. *Phys. Rept.*, 68:189–398, 1981.

[121] Marcus T. Grisaru, H. N. Pendleton, and P. van Nieuwenhuizen. Supergravity and the S Matrix. *Phys. Rev. D*, 15:996, 1977.

[122] Bernard de Wit and Daniel Z. Freedman. On SO(8) Extended Supergravity. *Nucl. Phys. B*, 130:105–113, 1977.

[123] C. R. Hagen and L. P. S. Singh. SEARCH FOR CONSISTENT INTERACTIONS OF THE RARITA-SCHWINGER FIELD. *Phys. Rev. D*, 26:393–398, 1982.

[124] Massimo Porrati and Rakibur Rahman. Causal Propagation of a Charged Spin 3/2 Field in an External Electromagnetic Background. *Phys. Rev. D*, 80:025009, 2009.

[125] V. Pascalutsa. Quantization of an interacting spin - 3 / 2 field and the Delta isobar. *Phys. Rev. D*, 58:096002, 1998.

[126] Vladimir Pascalutsa and Rob Timmermans. Field theory of nucleon to higher spin baryon transitions. *Phys. Rev. C*, 60:042201, 1999.

[127] V. Pascalutsa. Correspondence of consistent and inconsistent spin - 3/2 couplings via the equivalence theorem. *Phys. Lett. B*, 503:85–90, 2001.

[128] D Badagnani, C Barbero, and A Mariano. Consistence between πN Δ spin-3/2 gauge couplings and electromagnetic gauge invariance. 42(12):125001, nov 2015.

[129] D Badagnani, A Mariano, and C Barbero. Inconsistency of the spin-3/2 gauge invariant interaction of RaritaSchwinger fields. *Journal of Physics G: Nuclear and Particle Physics*, 44(2):025001, jan 2017.

[130] Eugene P. Wigner. On Unitary Representations of the Inhomogeneous Lorentz Group. *Annals Math.*, 40:149–204, 1939.

[131] Steven Weinberg. Feynman rules for any spin. *Phys. Rev.*, 133:B1318–B1332, Mar 1964.

[132] F. J. Dyson. The Radiation theories of Tomonaga, Schwinger, and Feynman. *Phys. Rev.*, 75:486–502, 1949.

[133] Juan Carlos Criado, Niko Koivunen, Martti Raidal, and Hardi Veermäe. Dark matter of any spin – an effective field theory and applications. *Phys. Rev. D*, 102(12):125031, 2020.

[134] Michael Edward Peskin and Daniel V. Schroeder. *An Introduction to Quantum Field Theory*. Westview Press, 1995. Reading, USA: Addison-Wesley (1995) 842 p.

[135] Juan C. Criado, Abdelhak Djouadi, Niko Koivunen, Martti Raidal, and Hardi Veermäe. Higher-spin particles at high-energy colliders. *JHEP*, 05:254, 2021.

[136] Juan C. Criado, Abdelhak Djouadi, Niko Koivunen, Kristjan Müürsepp, Martti Raidal, and Hardi Veermäe. Confronting spin-3/2 and other new fermions with the muon g-2 measurement. *Phys. Lett. B*, 820:136491, 2021.

[137] T. D. Lee and G. C. Wick. Finite Theory of Quantum Electrodynamics. *Phys. Rev. D*, 2:1033–1048, 1970.

[138] T. D. Lee and G. C. Wick. Questions of Lorentz Invariance in Field Theories With Indefinite Metric. *Phys. Rev. D*, 3:1046–1047, 1971.

Publications

Curriculum Vitae

Name:	Kristjan Müürsepp
Date and place of birth:	December 9, 1993, Rakvere, Estonia
Citizenship:	Estonian
Address:	National Institute of Chemical Physics and Biophysics, Rävala 10, Tallinn 10143, Estonia
E-mail:	kristjan.muursepp@kbfi.ee, kristjam@ut.ee

Education

2020-2024	PhD student, theoretical physics National Institute of Chemical Physics and Biophysics, University of Tartu
2018-2020	MSc, theoretical physics, University of Tartu
2013-2017	BSc, mathematics and physics, University of Aberdeen
2010-2013	Hugo Treffner Gymnasium

Elulookirjeldus

Nimi:	Kristjan Müürsepp
Sünniaeg ja koht:	9. detsember, 1993, Rakvere, Eesti
Kodakondsus:	Eesti
Aadress:	Keemilise ja Bioloogilise Füüsika Instituut, Rävala 10, Tallinn 10143, Eesti
E-post:	kristjan.muursepp@kbfi.ee, kristjam@ut.ee

Haridus

2020-2024	PhD, teoreetiline füüsika Keemilise ja Bioloogilise Füüsika Instituut, Tartu Ülikool
2018-2020	MSc Teoreetiline Füüsika Tartu Ülikool
2013-2017	BSc, Füüsika Aberdeeni Ülikool
2010-2013	Hugo Treffneri Gümnaasium

DISSERTATIONES PHYSICAE UNIVERSITATIS TARTUENSIS

1. **Andrus Ausmees.** XUV-induced electron emission and electron-phonon interaction in alkali halides. Tartu, 1991.
2. **Heiki Sõnajalg.** Shaping and recalling of light pulses by optical elements based on spectral hole burning. Tartu, 1991.
3. **Sergei Savihhin.** Ultrafast dynamics of F-centers and bound excitons from picosecond spectroscopy data. Tartu, 1991.
4. **Ergo Nõmmiste.** Leelishalogeniidide röntgenelektronemissioon kiiritamisel footonitega energiaga 70–140 eV. Tartu, 1991.
5. **Margus Rätsep.** Spectral gratings and their relaxation in some low-temperature impurity-doped glasses and crystals. Tartu, 1991.
6. **Tõnu Pullerits.** Primary energy transfer in photosynthesis. Model calculations. Tartu, 1991.
7. **Olev Saks.** Attoampri diapasoonis voolude mõõtmise füüsikalised alused. Tartu, 1991.
8. **Andres Virro.** AlGaAsSb/GaSb heterostructure injection lasers. Tartu, 1991.
9. **Hans Korge.** Investigation of negative point discharge in pure nitrogen at atmospheric pressure. Tartu, 1992.
10. **Jüri Maksimov.** Nonlinear generation of laser VUV radiation for high-resolution spectroscopy. Tartu, 1992.
11. **Mark Aizengendler.** Photostimulated transformation of aggregate defects and spectral hole burning in a neutron-irradiated sapphire. Tartu, 1992.
12. **Hele Siimon.** Atomic layer molecular beam epitaxy of A^2B^6 compounds described on the basis of kinetic equations model. Tartu, 1992.
13. **Tõnu Reinot.** The kinetics of polariton luminescence, energy transfer and relaxation in anthracene. Tartu, 1992.
14. **Toomas Rõõm.** Paramagnetic H^{2-} and F^{+} centers in CaO crystals: spectra, relaxation and recombination luminescence. Tallinn, 1993.
15. **Erko Jalviste.** Laser spectroscopy of some jet-cooled organic molecules. Tartu, 1993.
16. **Alvo Aabloo.** Studies of crystalline celluloses using potential energy calculations. Tartu, 1994.
17. **Peeter Paris.** Initiation of corona pulses. Tartu, 1994.
18. **Павел Рубин.** Локальные дефектные состояния в CuO_2 плоскостях высокотемпературных сверхпроводников. Тарту, 1994.
19. **Olavi Ollikainen.** Applications of persistent spectral hole burning in ultrafast optical neural networks, time-resolved spectroscopy and holographic interferometry. Tartu, 1996.
20. **Ülo Mets.** Methodological aspects of fluorescence correlation spectroscopy. Tartu, 1996.
21. **Mikhail Danilkin.** Interaction of intrinsic and impurity defects in CaS:Eu luminophors. Tartu, 1997.

22. **Ирина Кудрявцева.** Создание и стабилизация дефектов в кристаллах KBr, KCl, RbCl при облучении ВУФ-радиацией. Тарту, 1997.
23. **Andres Osvet.** Photochromic properties of radiation-induced defects in diamond. Tartu, 1998.
24. **Jüri Örd.** Classical and quantum aspects of geodesic multiplication. Tartu, 1998.
25. **Priit Sarv.** High resolution solid-state NMR studies of zeolites. Tartu, 1998.
26. **Сергей Долгов.** Электронные возбуждения и дефектообразование в некоторых оксидах металлов. Тарту, 1998.
27. **Kaupo Kukli.** Atomic layer deposition of artificially structured dielectric materials. Tartu, 1999.
28. **Ivo Heinmaa.** Nuclear resonance studies of local structure in $RBa_2Cu_3O_{6+x}$ compounds. Tartu, 1999.
29. **Aleksander Shelkan.** Hole states in CuO_2 planes of high temperature superconducting materials. Tartu, 1999.
30. **Dmitri Nevedrov.** Nonlinear effects in quantum lattices. Tartu, 1999.
31. **Rein Ruus.** Collapse of 3d (4f) orbitals in 2p (3d) excited configurations and its effect on the x-ray and electron spectra. Tartu, 1999.
32. **Valter Zazubovich.** Local relaxation in incommensurate and glassy solids studied by Spectral Hole Burning. Tartu, 1999.
33. **Indrek Reimand.** Picosecond dynamics of optical excitations in GaAs and other excitonic systems. Tartu, 2000.
34. **Vladimir Babin.** Spectroscopy of exciton states in some halide macro- and nanocrystals. Tartu, 2001.
35. **Toomas Plank.** Positive corona at combined DC and AC voltage. Tartu, 2001.
36. **Kristjan Leiger.** Pressure-induced effects in inhomogeneous spectra of doped solids. Tartu, 2002.
37. **Helle Kaasik.** Nonperturbative theory of multiphonon vibrational relaxation and nonradiative transitions. Tartu, 2002.
38. **Tõnu Laas.** Propagation of waves in curved spacetimes. Tartu, 2002.
39. **Rünno Lõhmus.** Application of novel hybrid methods in SPM studies of nanostructural materials. Tartu, 2002.
40. **Kaido Reivelt.** Optical implementation of propagation-invariant pulsed free-space wave fields. Tartu, 2003.
41. **Heiki Kasemägi.** The effect of nanoparticle additives on lithium-ion mobility in a polymer electrolyte. Tartu, 2003.
42. **Villu Repän.** Low current mode of negative corona. Tartu, 2004.
43. **Алексей Котлов.** Оксианионные диэлектрические кристаллы: зонная структура и электронные возбуждения. Tartu, 2004.
44. **Jaak Talts.** Continuous non-invasive blood pressure measurement: comparative and methodological studies of the differential servo-oscillometric method. Tartu, 2004.
45. **Margus Saal.** Studies of pre-big bang and braneworld cosmology. Tartu, 2004.

46. **Eduard Gerškevitš.** Dose to bone marrow and leukaemia risk in external beam radiotherapy of prostate cancer. Tartu, 2005.
47. **Sergey Shchemelyov.** Sum-frequency generation and multiphoton ionization in xenon under excitation by conical laser beams. Tartu, 2006.
48. **Valter Kiisk.** Optical investigation of metal-oxide thin films. Tartu, 2006.
49. **Jaan Aarik.** Atomic layer deposition of titanium, zirconium and hafnium dioxides: growth mechanisms and properties of thin films. Tartu, 2007.
50. **Astrid Rekker.** Colored-noise-controlled anomalous transport and phase transitions in complex systems. Tartu, 2007.
51. **Andres Punning.** Electromechanical characterization of ionic polymer-metal composite sensing actuators. Tartu, 2007.
52. **Indrek Jõgi.** Conduction mechanisms in thin atomic layer deposited films containing TiO_2. Tartu, 2007.
53. **Aleksei Krasnikov.** Luminescence and defects creation processes in lead tungstate crystals. Tartu, 2007.
54. **Küllike Rägo.** Superconducting properties of MgB_2 in a scenario with intra- and interband pairing channels. Tartu, 2008.
55. **Els Heinsalu.** Normal and anomalously slow diffusion under external fields. Tartu, 2008.
56. **Kuno Kooser.** Soft x-ray induced radiative and nonradiative core-hole decay processes in thin films and solids. Tartu, 2008.
57. **Vadim Boltrushko.** Theory of vibronic transitions with strong nonlinear vibronic interaction in solids. Tartu, 2008.
58. **Andi Hektor.** Neutrino Physics beyond the Standard Model. Tartu, 2008.
59. **Raavo Josepson.** Photoinduced field-assisted electron emission into gases. Tartu, 2008.
60. **Martti Pärs.** Study of spontaneous and photoinduced processes in molecular solids using high-resolution optical spectroscopy. Tartu, 2008.
61. **Kristjan Kannike.** Implications of neutrino masses. Tartu, 2008.
62. **Vigen Issahhanjan.** Hole and interstitial centres in radiation-resistant MgO single crystals. Tartu, 2008.
63. **Veera Krasnenko.** Computational modeling of fluorescent proteins. Tartu, 2008.
64. **Mait Müntel.** Detection of doubly charged higgs boson in the CMS detector. Tartu, 2008.
65. **Kalle Kepler.** Optimisation of patient doses and image quality in diagnostic radiology. Tartu, 2009.
66. **Jüri Raud.** Study of negative glow and positive column regions of capillary HF discharge. Tartu, 2009.
67. **Sven Lange.** Spectroscopic and phase-stabilisation properties of pure and rare-earth ions activated ZrO_2 and HfO_2. Tartu, 2010.
68. **Aarne Kasikov.** Optical characterization of inhomogeneous thin films. Tartu, 2010.
69. **Heli Valtna-Lukner.** Superluminally propagating localized optical pulses. Tartu, 2010.

70. **Artjom Vargunin.** Stochastic and deterministic features of ordering in the systems with a phase transition. Tartu, 2010.
71. **Hannes Liivat.** Probing new physics in e+e− annihilations into heavy particles via spin orientation effects. Tartu, 2010.
72. **Tanel Mullari.** On the second order relativistic deviation equation and its applications. Tartu, 2010.
73. **Aleksandr Lissovski.** Pulsed high-pressure discharge in argon: spectroscopic diagnostics, modeling and development. Tartu, 2010.
74. **Aile Tamm.** Atomic layer deposition of high-permittivity insulators from cyclopentadienyl-based precursors. Tartu, 2010.
75. **Janek Uin.** Electrical separation for generating standard aerosols in a wide particle size range. Tartu, 2011.
76. **Svetlana Ganina.** Hajusandmetega ülesanded kui üks võimalus füüsikaõppe efektiivsuse tõstmiseks. Tartu, 2011
77. **Joel Kuusk.** Measurement of top-of-canopy spectral reflectance of forests for developing vegetation radiative transfer models. Tartu, 2011.
78. **Raul Rammula**. Atomic layer deposition of HfO_2 – nucleation, growth and structure development of thin films. Tartu, 2011.
79. **Сергей Наконечный.** Исследование электронно-дырочных и интерстициал-вакансионных процессов в монокристаллах MgO и LiF методами термоактивационной спектроскопии. Тарту, 2011.
80. **Niina Voropajeva.** Elementary excitations near the boundary of a strongly correlated crystal. Tartu, 2011.
81. **Martin Timusk.** Development and characterization of hybrid electro-optical materials. Tartu, 2012, 106 p.
82. **Merle Lust.** Assessment of dose components to Estonian population. Tartu, 2012, 84 p.
83. **Karl Kruusamäe.** Deformation-dependent electrode impedance of ionic electromechanically active polymers. Tartu, 2012, 128 p.
84. **Liis Rebane.** Measurement of the $W \to \tau\nu$ cross section and a search for a doubly charged Higgs boson decaying to τ-leptons with the CMS detector. Tartu, 2012, 156 p.
85. **Jevgeni Šablonin.** Processes of structural defect creation in pure and doped MgO and NaCl single crystals under condition of low or super high density of electronic excitations. Tartu, 2013, 145 p.
86. **Riho Vendt**. Combined method for establishment and dissemination of the international temperature scale. Tartu, 2013, 108 p.
87. **Peeter Piksarv.** Spatiotemporal characterization of diffractive and non-diffractive light pulses. Tartu, 2013, 156 p.
88. **Anna Šugai.** Creation of structural defects under superhigh-dense irradiation of wide-gap metal oxides. Tartu, 2013, 108 p.
89. **Ivar Kuusik.** Soft X-ray spectroscopy of insulators. Tartu, 2013, 113 p.
90. **Viktor Vabson**. Measurement uncertainty in Estonian Standard Laboratory for Mass. Tartu, 2013, 134 p.

91. **Kaupo Voormansik.** X-band synthetic aperture radar applications for environmental monitoring. Tartu, 2014, 117 p.
92. **Deivid Pugal.** hp-FEM model of IPMC deformation. Tartu, 2014, 143 p.
93. **Siim Pikker.** Modification in the emission and spectral shape of photostable fluorophores by nanometallic structures. Tartu, 2014, 98 p.
94. **Mihkel Pajusalu**. Localized Photosynthetic Excitons. Tartu, 2014, 183 p.
95. **Taavi Vaikjärv.** Consideration of non-adiabaticity of the Pseudo-Jahn-Teller effect: contribution of phonons. Tartu, 2014, 129 p.
96. **Martin Vilbaste.** Uncertainty sources and analysis methods in realizing SI units of air humidity in Estonia. Tartu, 2014, 111 p.
97. **Mihkel Rähn.** Experimental nanophotonics: single-photon sources- and nanofiber-related studies. Tartu, 2015, 107 p.
98. **Raul Laasner.** Excited state dynamics under high excitation densities in tungstates. Tartu, 2015, 125 p.
99. **Andris Slavinskis.** EST Cube-1 attitude determination. Tartu, 2015, 104 p.
100. **Karlis Zalite**. Radar Remote Sensing for Monitoring Forest Floods and Agricultural Grasslands. Tartu, 2016, 124 p.
101. **Kaarel Piip.** Development of LIBS for *in-situ* study of ITER relevant materials. Tartu, 2016, 93 p.
102. **Kadri Isakar.** ^{210}Pb in Estonian air: long term study of activity concentrations and origin of radioactive lead. Tartu, 2016, 107 p.
103. **Artur Tamm.** High entropy alloys: study of structural properties and irradiation response. Tartu, 2016, 115 p.
104. **Rasmus Talviste.** Atmospheric-pressure He plasma jet: effect of dielectric tube diameter. Tartu, 2016, 107 p.
105. **Andres Tiko.** Measurement of single top quark properties with the CMS detector. Tartu, 2016, 161 p.
106. **Aire Olesk.** Hemiboreal Forest Mapping with Interferometric Synthetic Aperture Radar. Tartu, 2016, 121 p.
107. **Fred Valk.** Nitrogen emission spectrum as a measure of electric field strength in low-temperature gas discharges. Tartu, 2016, 149 p.
108. **Manoop Chenchiliyan.** Nano-structural Constraints for the Picosecond Excitation Energy Migration and Trapping in Photosynthetic Membranes of Bacteria. Tartu, 2016, 115p.
109. **Lauri Kaldamäe.** Fermion mass and spin polarisation effects in top quark pair production and the decay of the higgs boson. Tartu, 2017, 104 p.
110. **Marek Oja.** Investigation of nano-size α- and transition alumina by means of VUV and cathodoluminescence spectroscopy. Tartu, 2017, 89 p.
111. **Viktoriia Levushkina.** Energy transfer processes in the solid solutions of complex oxides. Tartu, 2017, 101 p.
112. **Mikk Antsov.** Tribomechanical properties of individual 1D nanostructures: experimental measurements supported by finite element method simulations. Tartu, 2017, 101 p.
113. **Hardi Veermäe.** Dark matter with long range vector-mediated interactions. Tartu, 2017, 137 p.

114. **Aris Auzans.** Development of computational model for nuclear energy systems analysis: natural resources optimisation and radiological impact minimization. Tartu, 2018, 138 p.
115. **Aleksandr Gurev**. Coherent fluctuating nephelometry application in laboratory practice. Tartu, 2018, 150 p.
116. **Ardi Loot**. Enhanced spontaneous parametric downconversion in plasmonic and dielectric structures. Tartu, 2018, 164 p.
117. **Andreas Valdmann.** Generation and characterization of accelerating light pulses. Tartu, 2019, 85 p.
118. **Mikk Vahtrus.** Structure-dependent mechanical properties of individual one-dimensional metal-oxide nanostructures. Tartu, 2019, 110 p.
119. **Ott Vilson.** Transformation properties and invariants in scalar-tensor theories of gravity. Tartu, 2019, 183 p.
120. **Indrek Sünter.** Design and characterisation of subsystems and software for ESTCube-1 nanosatellite. Tartu, 2019, 195 p.
121. **Marko Eltermann**. Analysis of samarium doped TiO_2 optical and multi-response oxygen sensing capabilities. Tartu, 2019, 113 p.
122. **Kalev Erme**. The effect of catalysts in plasma oxidation of nitrogen oxides. Tartu, 2019, 114 p.
123. **Sergey Koshkarev.** A phenomenological feasibility study of the possible impact of the intrinsic heavy quark (charm) mechanism on the production of doubly heavy mesons and baryons. Tartu, 2020, 134 p.
124. **Kristi Uudeberg.** Optical Water Type Guided Approach to Estimate Water Quality in Inland and Coastal Waters. Tartu, 2020, 222 p.
125. **Daniel Blixt.** Hamiltonian analysis of covariant teleparallel theories of gravity. Tartu, 2021, 142 p.
126. **Ulbossyn Ualikhanova.** Gravity theories based on torsion: theoretical and observational constraints. Tartu, 2021, 154 p.
127. **Iaroslav Iakubivskyi**. Nanospacecraft for Technology Demonstration and Science Missions. Tartu, 2021, 177 p.
128. **Heido Trofimov.** Polluted clouds at air pollution hot spots help to better understand anthropogenic impacts on Earth's climate. Tartu, 2022, 96 p.
129. **Ott Rebane.** *In situ* non-contact sensing of microbiological contamination by fluorescence spectroscopy. Tartu, 2022, 157 p.
130. **Juhan Saaring.** Ultrafast Relaxation Processes in Ternary Hexafluorides Studied under Synchrotron Radiation Excitation. Tartu, 2022, 106 p.
131. **Ahmet Ilker Topuz.** Quantitative and qualitative investigations for muon scattering tomography via GEANT4 simulations: A computational study. Tartu, 2023, 163 p.
132. **Nico Benincasa.** Phase transitions and gravitational waves in models of dark matter. Tartu, 2023, 206 p.
133. **Kaja Pae.** Electron-phonon interactions in local degenerate electronic states in solids. Tartu, 2024, 201 p.